



Temporal Characteristics and Atmospheric Drivers of Onsets and Terminations of Soil Moisture Droughts in Europe

Woon Mi Kim¹, Santos J. González-Rojí^{2,3}, Isla R. Simpson¹, and Daniel Kennedy^{1,4}

¹Climate and Global Dynamics Laboratory, NSF National Center for Atmospheric Research, Boulder CO, United States

²Climate and Environmental Physics, University of Bern, Bern, Switzerland

³Oeschger Centre for Climate Change Research, University of Bern, Bern, Switzerland

⁴Earth Research Institute, University of California, Santa Barbara CA, United States

Correspondence: Woon Mi Kim (wmikim@ucar.edu)

Abstract.

Many studies have focused on understanding the drivers of soil moisture droughts in Europe when the events have already intensified. Still, how atmospheric circulation changes throughout the entire life cycle of droughts, particularly during the transition periods to drought initiation and termination, has not been thoroughly investigated. Therefore, this study investigates temporal characteristics and atmospheric circulation associated with onsets (a transition period from a normal condition to drought) and terminations (a transition period from drought to a normal condition) of soil moisture droughts in Europe during 1980–2020. The typical duration, preferred seasons of occurrence, and atmospheric circulation during onsets and terminations are examined. The regions of study are central (CEU) and Mediterranean (MED) Europe, and soil moisture from ERA5-Land, GLEAM version 3, SoMo.ml, Noah-LSM, and a simulation from the Community Land Model version 5 (CLM-TRENDY) are utilized.

Our findings indicate that the duration of onsets and terminations depends on the dataset: the five soil moisture datasets exhibit different mean duration of onsets and terminations, with ERA5-Land showing shorter and GLEAM longer duration across Europe. Nevertheless, within the same dataset, onsets and terminations exhibit similar durations, implying that onsets and terminations can occur at the same speed. Regarding the preferred seasons for onsets and terminations, onsets occur more during the wet seasons, specifically summer in CEU and autumn and winter in MED. Nevertheless, the frequencies of occurrence during these seasons only slightly exceed that during other seasons. Terminations tend to occur more during the driest seasons. For atmospheric circulation, onsets come with large-scale anticyclonic atmospheric circulation patterns. Terminations do not exhibit a dominant mean circulation pattern over the region where terminations occur but instead show geopotential height anomalies with reduced magnitudes in Europe and a high-pressure system over the North Atlantic. The anticyclonic circulation during onsets is anomalously persistent and shows linkages with the North Atlantic Oscillation (NAO). Positive NAO occurs much more frequently during onsets compared to other drought phases. This finding implies an important role for this large-scale mode of variability in initiating dry periods by reducing soil moisture and its potential to serve as an early warning for droughts during the period prior to the events.



1 Introduction

25 Drought is a climate phenomenon that is characterized by a prolonged period of dry conditions (Dai, 2011). When depletion of water occurs in the soil, the event is referred to as a soil moisture drought. Soil moisture droughts can result from a persistent dry period with little precipitation (meteorological drought) alone or can arise from the combined influence of reduced precipitation and increased evapotranspiration. The impacts of soil moisture droughts can be far-reaching, affecting ecosystems and a wide range of socioeconomic sectors (Naumann et al., 2015; Bachmair et al., 2016) with clearly apparent impacts on agricultural activities (Moravec et al., 2021). The damage caused by droughts becomes increasingly severe with the increasing duration of the events. Although dry-wet fluctuations are a natural aspect of a region's hydroclimate, there is evidence that anthropogenic warming has perturbed the natural characteristics of droughts through an increase in vapor pressure deficit and the intensification of the global hydrological cycle (Trenberth, 2011; Van Loon et al., 2016; Seneviratne et al., 2021).

Determining the precise timing of initiation and termination of droughts is challenging, primarily due to the complex and multifaceted nature of droughts (Cook et al., 2018). The drivers of a drought can be diverse, from large-scale climate patterns to regional-scale processes, including synoptic weather systems and land-atmosphere interactions. Each of these processes has different time scales of influence on soil moisture variability. Another complexity arises from the fact that droughts are typically slow events, whose impacts on the ecosystem become noticeable when the events have already reached the mature phase, with some accumulated periods of precipitation or soil moisture deficit (Wilhite, 2000). These factors collectively make it challenging to define when exactly a dry or wet condition that initiated or ended a drought has commenced. However, investigating drought phases, particularly periods of transitions to drought onsets and terminations, is a topic that requires more attention to improve early predictions of such events and prepare suitable mitigation strategies.

Several studies that investigated the life cycle of droughts have defined drought phases based on different standardized drought indices, accumulated precipitation deficit, or soil moisture anomalies (e.g., Mo, 2011; Seager et al., 2019; Shah and Mishra, 2020; Řehoř et al., 2021). Although the criteria to divide the life cycle of a drought into different phases vary across the studies, in general, a drought initiation is the period preceding a drought threshold, and a drought termination is the recovery period from the drought threshold or from the minimum soil moisture or precipitation deficit to normal conditions. The typical duration of drought phases and the drivers involved in these different phases of the drought life cycle have been investigated in these studies.

50 Focusing on the United States, Mo (2011) examined the duration and large-scale drivers associated with onsets and terminations of meteorological and soil moisture droughts on various time scales across the United States using the North American Land Data Assimilation System (NLDAS-1) dataset during 1916–2007. This study shows that drought onsets are slower than terminations, as onsets require a certain accumulation period of precipitation deficits until they can progress into droughts, whereas heavy precipitation events can more easily alleviate drought. Due to a longer development period, onsets are expected to be more predictable than terminations. In contrast, using the models from NLDAS-2, Seager et al. (2019) showed that over the southern Great Plains, there is no difference in the duration between onsets and terminations of soil moisture droughts on a seasonal time scale. They suggest that this mismatch in the duration between these two studies may arise from the use of

different definitions of onsets and terminations. Mo (2011) defined onsets (or the transition periods to onsets) as all preceding months with a precipitation deficit in the year prior to reaching the drought threshold. Seager et al. (2019) considered onsets as transition periods from normal (above a negative unit standard deviation of soil moisture anomalies) to below the drought threshold (below a negative unit standard deviation of soil moisture anomalies, with the change over the season greater than one standard deviation). Still, both studies found that large-scale atmosphere-ocean climate anomalies in the tropics are the drivers of onsets and terminations of droughts.

For other regions, Shah and Mishra (2020) investigated characteristics of onsets and terminations of different types of droughts in India based on the soil moisture and surface datasets from the Variable Infiltration Capacity (VIC) model. Onsets and terminations of droughts in India tend to occur more frequently during the summer monsoon seasons, and their long-term variability is linked with El Niño Southern Oscillations (ENSO) and Indian Ocean Dipole (IOD). For Europe, Řehoř et al. (2021) examined atmospheric circulation anomalies associated with the three phases of soil moisture droughts in the Czech and Slovak Republics during 1961–2019. Using the output from the SoilClim model, they found that anticyclonic circulation types linked with low precipitation occur more frequently during the initiation (onsets) and throughout droughts. They found that the opposite cyclonic circulation types that bring precipitation to the region were more frequently observed during the recovery phase of droughts. Focusing on the British Isles, Parry et al. (2016) reviewed drought terminations in different studies, describing the various synoptic phenomena that end drought events in Europe.

In the last decade, Europe has experienced multiple intense droughts, marked by low soil moisture and accompanied by record-breaking summer heatwaves (e.g., Hari et al., 2020; Sousa et al., 2020; Moravec et al., 2021; Rakovec et al., 2022). Various studies have examined the drivers of individual droughts during this period. For example, the intense summer 2015 (Ionita et al., 2017) and 2018 (Moravec et al., 2021) droughts were driven by upper-level ridges and blocking highs, which were associated with a weakening of the subtropical jets. The 2016/2017 drought that affected almost the entire Europe was characterized by consecutive blocking events and subtropical ridges, which in turn weakened zonal circulation and moisture transport from the Atlantic (García-Herrera et al., 2019). During this drought event, the impact of temperature that drove an increase in atmospheric evaporative demand was more pronounced in southern Europe, and a similar situation was found for the 2022 event (Faranda et al., 2023). Vicente-Serrano et al. (2021) have indicated that the contribution of vapor pressure deficit on droughts has significantly increased in western Europe since the mid-20th century.

Despite these significant advances in the understanding of soil moisture droughts and drivers of the individual events presented above, the climatological characteristics of drought onsets and terminations in Europe are still a relatively under-explored topic. Climatological analyses of droughts have been conducted using standardized drought indices (e.g., Lloyd-Hughes and Saunders, 2002; Spinoni et al., 2015), but they did not focus on the characteristics of each of the drought phases. Thus, there is a need to improve understanding of the temporal characteristics and the atmospheric circulation patterns involved in the different phases of soil moisture droughts in Europe, particularly during onsets and terminations, to enhance early predictions and readiness for such extreme events.

The objective of this study is to investigate temporal characteristics of onsets and terminations and typical circulation patterns of soil moisture droughts in Europe during 1980–2020. First, we examine the climatological duration and preferred seasons of



occurrence of drought onsets and terminations. We also assess the relationship between the duration of onsets, terminations, and droughts, aiming to understand whether long (short) droughts require long (short) transition periods to begin or to recover
95 from. Aspects of the surface water balance (precipitation, precipitation minus evaporation, and soil moisture) involved in this relationship are also assessed.

Second, we analyze typical atmospheric circulation patterns of soil moisture drought onsets and terminations. One of the aims is to understand atmospheric processes that help onsets progress into droughts in CEU and MED. Then, particular focus is given to the association of different drought phases with the North Atlantic Oscillation (NAO) to address the large-scale
100 influence on drought phases and whether NAO serves as an early warning for soil moisture droughts in Europe.

The study regions are central (CEU) and Mediterranean Europe (MED), confined approximately between 45°N – 56.5°N and 9.5°W – 25.5°E for CEU and between 36.5°N – 45°N and 9.5°W – 25.5°E for MED following the division based on the IPCC climate reference regions (Iturbide et al., 2020). These are the regions in Europe that have been most affected by droughts in the last decade and where soil dryness is expected to increase in future warming scenarios, with medium (in central Europe)
105 and high (in southern Europe) confidence levels (Seneviratne et al., 2021).

The typical duration and seasonality of onsets and terminations are estimated using five soil moisture datasets. As most of the previous literature has employed only one soil moisture dataset or datasets from a single project, by using several soil moisture datasets from diverse projects, we aim to examine the robustness of the temporal characteristics of drought. The description of the datasets is given in Section 2. The definition of drought phases and other methods employed in the analysis
110 are introduced in Section 3. All the results on the climatological duration, seasonality of onsets and terminations, and typical circulation patterns are provided in Section 4. Finally, we present the discussion and conclusion in Section 5.

2 Data

Our study regions are central (CEU) and Mediterranean Europe (MED), extended approximately between 45°N – 56.5°N and 9.5°W – 25.5°E for CEU and between 36.5°N – 45°N and 9.5°W – 25.5°E for MED (Fig. 1c) based on the division following on
115 the IPCC climate reference regions (Iturbide et al., 2020). The analyzed period is 1980–2020.

The atmospheric variables we use are monthly averaged geopotential height at 500 hPa and precipitation obtained from the ERA5 (Hersbach et al., 2020) reanalysis. ERA5 is the latest reanalysis product of the European Centre for Medium-Range Weather Forecasts (ECMWF) and is generated with the 2016 version of the ECMWF numerical weather prediction model and the integrated forecasting system Cy41r2 data assimilation. The atmospheric variables have a horizontal resolution of $0.25^{\circ} \times$
120 0.25° , covering the period from 1940 until the present.

As an alternative precipitation dataset, we use E-OBS (version 27.0e; Cornes et al., 2018), which provides gridded daily precipitation amounts over Europe (land-only, 25°N – 71.5°N , 25°W – 45°E). E-OBS is based on weather station data collected by the ECA&D initiative (Klein Tank et al., 2002; Klok and Klein Tank, 2009), and the final precipitation values are generated as the means of an ensemble with 100 members of the daily precipitation estimates (Cornes et al., 2018). The spatial resolution
125 of E-OBS is $0.1^{\circ} \times 0.1^{\circ}$, and the data are available from 1950 onward.



We take Hurrell's station-based North Atlantic Oscillation Index (NAO) obtained from the NCAR climate data guide (Hurrell et al., 2023). The index represents the fluctuation between the Icelandic low and the Azores high, calculated as the difference of normalized sea level pressure (SLP) between the stations in Lisbon, Portugal and Stykkisholmur/Reykjavik, Iceland (Hurrell et al., 2003).

130 For soil moisture, we use five gridded products: three are the output of land surface models (LSM) forced by observation-based meteorological fields, one is based on a multi-layer soil model and assimilated with satellite-based products, and the last one is a machine-learning-trained observation-based dataset. The three soil moisture datasets from LSMs are ERA5-Land (Muñoz-Sabater et al., 2021), Noah-LSM (Koren et al., 1999) from the Global Land Data Assimilation System project (GLDAS; Rodell et al., 2004), and TRENDY (Friedlingstein et al., 2022) from the Community Land Model version 5 (CLM5; 135 Lawrence et al., 2019). The next dataset is Global Land Evaporation Amsterdam Model (GLEAM; Miralles et al., 2011; Martens et al., 2017) soil moisture, and the last one is SoMo.ml, which is derived from a machine learning-based model (O and Orth, 2021). Where available, evapotranspiration is also retrieved from these datasets for analysis.

We mostly rely on outputs from gridded datasets because our study requires continuous soil moisture data to identify drought phases properly, and many solely observation-based soil moisture datasets are generally short and not continuous in time and 140 space. The datasets are summarized in Table 1, and a brief description of each dataset follows.

ERA5-Land (Muñoz-Sabater et al., 2021) uses the offline ERA5 Land surface model, and it is forced by the atmospheric variables from the ERA5 reanalysis. The land processes are based on the ECMWF Scheme for Surface Exchanges over Land with land surface hydrology from the H-TESSEL model. The horizontal resolution is $0.25^\circ \times 0.25^\circ$, and we employ the data with the monthly time resolution.

145 GLEAM version 3 (Miralles et al., 2011; Martens et al., 2017) is a set of algorithms to estimate global evaporation that aims to provide an advanced representation of evaporation based on satellite and reanalysis forcing. The dataset contains not only terrestrial evaporation but also surface and root-zone soil moisture. Soil moisture is estimated using a multi-layer running-water balance model, and the upper-level soil moisture is assimilated with satellite-based microwave soil moisture. The spatial resolution of the dataset is $0.25^\circ \times 0.25^\circ$ covering the period 1980 to the present.

150 SoMo.ml v1 (SoMo; O and Orth, 2021) is a global daily soil moisture dataset reconstructed through a machine learning model trained with in-situ soil moisture measurements across the globe. SoMo employs a Long Short-Term Memory neural network to reconstruct the daily global soil moisture field. The predictors fed into the model are the meteorological variables from reanalysis and remote sensing datasets, and the target variable is soil moisture from 1000 in-situ measurements across the globe. The means and standard deviations of the daily in-situ soil moisture are scaled up to match those of the ERA5 grid 155 cells to produce seamless merging across different stations and time series. The horizontal resolution of SoMo is 0.25° , and the daily temporal resolution is converted to the monthly values by calculating the monthly averages. The temporal coverage of the dataset is from 2000 to 2019.

GLDAS (Rodell et al., 2004) is a project comprising various land surface models that provide global land surface variables. The output from GLDAS 2.1 is used for the period 2000–2020. The atmospheric input forcing for GLDAS combines data from 160 models and observations, including the Princeton meteorological forcing (Sheffield et al., 2006). From the LSMs that comprise



GLDAS, we use Noah LSM (Noah; Koren et al., 1999) that provides the surface level soil moisture. We employ the dataset with the spatial resolution of $1^\circ \times 1^\circ$ and the monthly average temporal resolution.

TRENDY (CLM-TRENDY) is a simulation from the offline CLM5 (Lawrence et al., 2019) and is part of the Global Carbon Budget 2022 project (Friedlingstein et al., 2022). The simulation was performed with a transient CO_2 and land use change from 1701 to 2021, and forced by the merged Climate Research Unit (CRU) – Japanese 55-year Reanalysis (JRA55) atmospheric forcing from 1901 onward. Before 1901, the atmospheric forcing during 1901–1920 is cycled over to fill the period. The dataset has a spatial resolution of approximately $0.95^\circ \times 1.25^\circ$ and the monthly temporal resolution.

Table 1. Soil moisture datasets employed in this study.

Dataset name (Abbreviation)	Institution	Type	Temporal resolution	Horizontal resolution	Reference
ERA5-Land (ERA5-Land)	ECMWF	Offline LSM	1950–Present	$0.25^\circ \times 0.25^\circ$	Muñoz-Sabater et al. (2021)
GLEAM v3 (GLEAM)	ESA	Multi-layer soil model and assimilated	1980–2021	$0.25^\circ \times 0.25^\circ$	Miralles et al. (2011) Martens et al. (2017)
SoMo.ml (SoMo)	MPI Biogeochemistry	Machine-learning trained model	2000–2019	$0.25^\circ \times 0.25^\circ$	O and Orth (2021)
Noah-LSM from GLDAS v2.1 (Noah)	NASA	Offline LSM	2000–Present	$1^\circ \times 1^\circ$	Rodell et al. (2004)
CLM-TRENDY (CLM-TRENDY)	NCAR	Offline LSM	1701–2021	$0.95^\circ \times 1.25^\circ$	Lawrence et al. (2019) Friedlingstein et al. (2022)

3 Methods

3.1 Metrics for soil moisture droughts

170 We use soil moisture from the surface level, which is 10 cm (SM10). This layer is chosen as it is the most commonly available among the datasets. GLEAM, SoMo, Noah, and CLM-TRENDY directly output 10 cm soil moisture. For ERA5-Land, as this level is not available, the corresponding value is obtained by estimating how much soil moisture is in the first 3 cm of the second layer (7–28 cm), then adding this amount onto the soil moisture of the first layer (7 cm). The assumption is that there is no gradient of soil moisture within the second layer.

175 Although the surface layer soil moisture cannot indicate dryness occurring in deeper soil layers, this depth is where soil moisture can be measured over a wide spatial extent and is commonly available in most soil moisture products. Moreover, SM10 is highly correlated to the commonly used operational drought indices, for instance, the Standardized Precipitation Evapotranspiration Index (SPEI; Vicente-Serrano et al., 2009). The variable is directly affected by changes in atmospheric circulation; hence, it is suitable for examining contemporaneous influences of atmospheric drivers on soil moisture.



180 The drought index to quantify soil moisture droughts is the three-month running mean of standardized surface soil moisture anomalies, same as Mo (2011). Running averages over three months smooth out noises in the monthly time series by taking into account the typical time scale of a season in the mid-latitudes. The anomalies are calculated at each grid point over the study regions. To obtain these soil moisture anomalies, first, the time series of soil moisture are deseasonalized through subtraction of the 2000–2014 (15 years) annual cycles, and then they are standardized using the multi-year standard deviations for each month
185 of the same period. These 15 years are used for standardization as they are common to all five datasets and exclude the intense soil moisture dryness in CEU that began in 2015. The three-month running means are calculated using these standardized soil moisture anomalies (from now on, denoted as ΔSM). These time series have a monthly time resolution, where an individual timestep t encompasses the soil moisture conditions over the previous three cumulative months, from t_{-2} to t_0 . For instance, the anomaly of February 1981 indicates the soil moisture conditions during December 1980–February 1981. This approach of
190 defining a drought index with a non-centralized moving average has an operational purpose, making it suitable for monitoring drought conditions for the current timestep. Additionally, this method aligns with other existing drought indices such as the Standardized Precipitation Index (SPI) (McKee et al., 1993) and SPEI.

3.2 Definitions of drought phases: onset, drought, and termination

We split the life cycle of drought into three phases: an onset (O), a drought (D), which is an intense dry period after the onset,
195 and a termination (T; O, D & T to refer to all three drought phases). In our study, onsets and transitions are the transition periods leading to droughts and to normal conditions, respectively. An entire O, D & T is composed of consecutive negative ΔSM with at least one ΔSM in timestep t (i.e., a 3-month average) falling below a minus one standard deviation (-1σ) during the drought. The entire phase then finishes with a positive ΔSM . The detailed definitions of each phase are the following, which are also illustrated in Fig 1a and b:

- 200 – An onset within a drought life cycle (an O, D & T) is a transition period from above zero ΔSM , without including this positive ΔSM , to a drought (ΔSM below -1σ). It is composed of the period prior to ΔSM falling below -1σ during which $-1\sigma < \Delta SM \leq 0$. This means that onset is the consecutive period of below normal (below zero) ΔSM prior to crossing a drought threshold (-1σ). In situations where a drought begins rapidly, with ΔSM falling below -1σ without any transition period with $-1\sigma < \Delta SM \leq 0$, the onset is said to have a duration of one-month timestep. This definition
205 ensures a minimum onset period of one month, taking into account the monthly resolution of ΔSM .
- A termination is defined as the period over which ΔSM transitions from below -1σ to above zero, without including the timestep with a positive ΔSM . It is a transition period from the end of a drought to a normal state. It is counted backward from the first time ΔSM exceeds zero after a drought event, back to the timestep after the most recent timestep with $\Delta SM < -1\sigma$. Similar to the onset, if there is no transition period with $-1\sigma < \Delta SM \leq 0$, then the duration of termination
210 is considered to be one month.



- A drought is the rest of the months within a drought life cycle excluding O&T. It commences with the first occurrence of $\Delta SM \leq -1\sigma$ and continues until the last timestep of the life cycle where $\Delta SM \leq -1\sigma$. ΔSM during this period must be negative but is not necessarily always below -1σ .
- Additionally, we define a no-drought dry period (NDD). This period is characterized by $-1\sigma < \Delta SM < 0$ without ever progressing into an actual drought with $\Delta SM \leq -1\sigma$ (Fig. 1b).

215

A drought threshold of -1σ in a standardized drought index defined in this study corresponds approximately to the 15.9th percentile level. Based on the classification of drought categories in other standardized drought indices such as SPI or SPEI (Lloyd-Hughes Benjamin and Saunders Mark A., 2002), values below this threshold indicate moderate to extreme droughts. Our definition of O & T follows a similar approach to that of Seager et al. (2019), with the same threshold of -1σ . But our analysis uses the drought metric with a monthly time scale, similarly as Mo (2011).

220

3.3 Temporal characteristics of droughts

We calculate the duration of onsets and terminations by counting the number of timesteps within the onsets or terminations for each drought event at each grid point in the study regions. Statistical assessment to compare the mean duration between onsets and terminations and to compare the duration of onsets and terminations between the datasets is performed using t-tests (Wilks, 2011) within CEU and MED separately. For this, the durations of all individual O&T are collected and separated into CEU and MED. For the t-tests, the null hypothesis assumes that the means of the two phases or two datasets are derived from the same population. Our test, therefore, assesses whether their means are inconsistent with being sampled from the same population at a 95% level using a two-sided test.

225

The preferred seasons for O&T's are estimated using ERA5-Land, GLEAM, and CLM-TRENDY since they cover a longer time period (1980–2020). Thus, we can include more drought events in that analysis. Since the study regions are located in the mid-latitudes, a standard division into the four boreal seasons is adopted (DJF is winter, MAM is spring, JJA is summer, and SON is fall). We estimate the preferred seasons of the last month of onset (the timestep before crossing -1σ) and the first month of termination (the timestep when ΔSM first crosses above -1σ within the termination). An onset (here, the last month of onsets) or termination (the first months of termination) is said to occur in a given season if it falls within that given season. The number of O&T's within a season is counted at each grid point, and then, the ratio between the number of onset (or termination) occurrences during a given season and the total onset (or termination) occurrences is calculated. If droughts occur uniformly across seasons, the occurrence ratio would be 0.25 for each season.

235

The preferred seasons for O&T's are also assessed on a continental scale, considering more subdivisions within CEU and MED. This is done to take into account different mean hydroclimate conditions within the region. For this purpose, the two study regions, CEU and MED, which are divided following Iturbide et al. (2020), are then separated into six, following similar divisions employed by Christensen and Christensen (2007) (Fig. 1c): Iberian Peninsula (IP), east-southern Europe (EMED), Alps (ALP), France (FR), mid-Europe (MCEU), and east-central Europe (ECEU). A median of the occurrence ratio of O&T in a season across the grid points over each subdivision is then calculated.

240

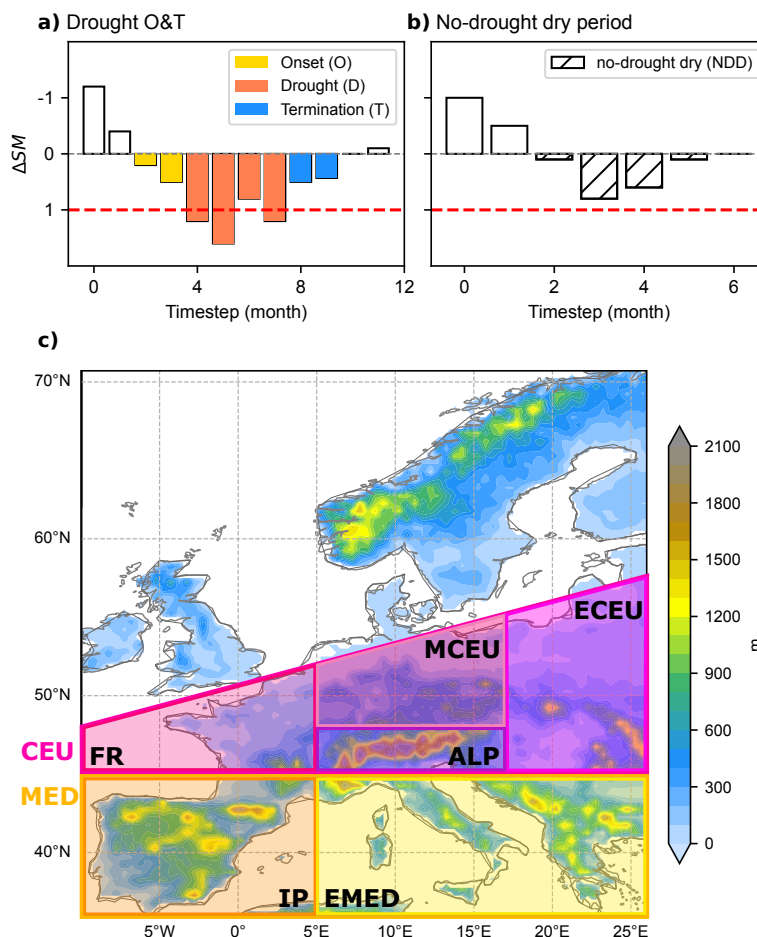


Figure 1. Illustration of drought phases based on the soil moisture anomaly (ΔSM): a) a complete drought life cycle O, D, & T, b) a no-drought dry period. Shaded in colors are the onset (O; yellow), drought (D; orange), and termination (T; blue). The red-dashed lines indicate the -1σ drought threshold. c) Topography in Europe and regional divisions based on Christensen and Christensen (2007) and Iturbide et al. (2020).

To examine the potential causes of discrepancies between the soil moisture datasets in representing the variability of ΔSM and drought phases, we compare evapotranspiration and precipitation from these datasets. For this, the monthly means of evapotranspiration and precipitation during the common period 2000–2020 are calculated over the study region, and also their anomalies are obtained by deseasonalizing the time series.

3.4 Relationship between the duration of drought phases, drought intensities, precipitation, evapotranspiration

To assess the relationship between the duration of onsets and droughts and between the duration of terminations and droughts, first, the duration of individual O&T events from the grid points over the study domain (CEU and MED together) are collected.



Then, the individual durations of onsets or terminations, d_{onset} or d_{term} , are grouped based on the same duration. The drought durations $d_{drought}$ within each onset group with $d_{onset} = i$ (or each termination group with $d_{term} = i$) are then spatially weighted and averaged. This results in a mean drought duration $\bar{d}_{drought}$ that belongs to $d_{onset} = i$ or $d_{term} = i$. For example, for the onsets, the mathematical expression for the spatially-weighted averaged mean drought duration $\bar{d}_{drought}$ for $d_{onset} = i$ is:

$$\bar{d}_{drought}(i) = \frac{\sum_{n=1}^N d_{drought}(n, i) * \cos(lat(n))}{\sum_{n=1}^N \cos(lat(n))} \quad n = 1, \dots, N; \quad i = 1, \dots, M \quad (1)$$

where $d_{drought}$ is the durations of the individual droughts with the onset duration i , with i ranging from 1 to the maximum duration M of onsets, N is the total number of grid points, and $lat(n)$ is the corresponding latitude for the grid point at location n . Eq. 1 is repeated for all i until M , resulting in a series of mean drought durations with M values. The same is repeated for drought durations for terminations. Here, instead of taking the common period among the datasets, the entire period of each dataset is used. Finally, $\bar{d}_{drought}$ and the O&T durations are compared.

Next, we assess the relationship between the O&T duration and the intensities of droughts to address whether intense droughts relate to the duration of onsets or termination. Drought intensities are estimated using the cumulative ΔSM that combines the mean decreases in ΔSM during droughts and the drought duration. The same Eq. 1 is repeated for all $d_{onset} = i$ and $d_{term} = i$, but replacing $d_{drought}$ by the cumulative ΔSM of drought events.

Lastly, we also examine how aspects of surface water balance, more specifically, precipitation (P), and precipitation minus evapotranspiration (P-E) are related to the O&T duration. Of particular interest is to identify whether the required net input water to initiate or terminate droughts depends on the duration of the transition periods, i.e., O&T. Alternative P and E datasets are used for those soil moisture products whose input P and resulting E are not openly available. For SoMo, P and E are taken from ERA5 and ERA5-Land, respectively. For GLEAM, P is obtained on the observation-based E-OBS, as the input forcing of GLEAM is a merged P from observation and satellite-based products.

Using these P and E, cumulative anomalies of P, ΔP , and P-E, $\Delta(P-E)$ associated with d_{onset} and d_{term} are estimated. ΔP and $\Delta(P-E)$ are obtained by deseasonalizing P and P-E with respect to 2000–2014. The spatial averages of cumulative ΔP and $\Delta(P-E)$ corresponding to $\bar{d}_{onset} = i$ or $\bar{d}_{term} = i$ are computed repeating Eq.1, replacing $d_{drought}$ by cumulative ΔP and $\Delta(P-E)$. The relationship between the mean duration of onsets or terminations, cumulative ΔP , and $\Delta(P-E)$ are assessed.

3.5 Circulation patterns and analysis of regional variables during drought phases

Atmospheric circulation patterns during O&T are depicted using anomalies of geopotential height at 500 hPa (ΔGP) from ERA5. ΔGP is obtained by deseasonalizing the monthly geopotential height with the 2000–2014 multi-year annual cycle. Then, three-month running means of the anomalies are calculated in the same manner as was done to obtain ΔSM .

We analyze atmospheric circulation anomalies during O&T's, considering O&T periods that the three soil moisture datasets, ERA5-Land, GLEAM, and CLM-TRENDY agree on during 1980–2020. When examining the atmospheric circulation, we focus on the atmospheric drivers of large-scale dryness, which affects the mean ΔSM of each subregion, as opposed to the



circulation patterns accompanying dryness at every grid point. Therefore, for this aspect of the analysis, O, T, and NDD are determined using the spatially averaged time series of ΔSM for each of the six subregions. Mean circulation during NDDs is examined to understand which atmospheric conditions help onsets to progress into droughts and not be dissipated before reaching droughts as dryness during NDDs.

Lastly, the mean NAO index associated with each drought phase and NDD is determined to assess the influence of this dominant circulation pattern in the Euro-Atlantic region on drought phases. Also, the Pearson correlation coefficient between the NAO index and ΔSM is estimated over the entire period and each season at each grid point.

290 4 Results and discussions

4.1 Temporal characteristics of drought onsets and terminations

The duration of onsets and terminations (O&T duration) of droughts are estimated during 2000–2019 for SoMo and 2000–2020 for the other four soil moisture datasets. The mean duration is presented in Fig. 2. The duration of ERA5-Land, GLEAM, and CLM-TRENDY during 1980–2020 is included in the supplement (Fig. S1).

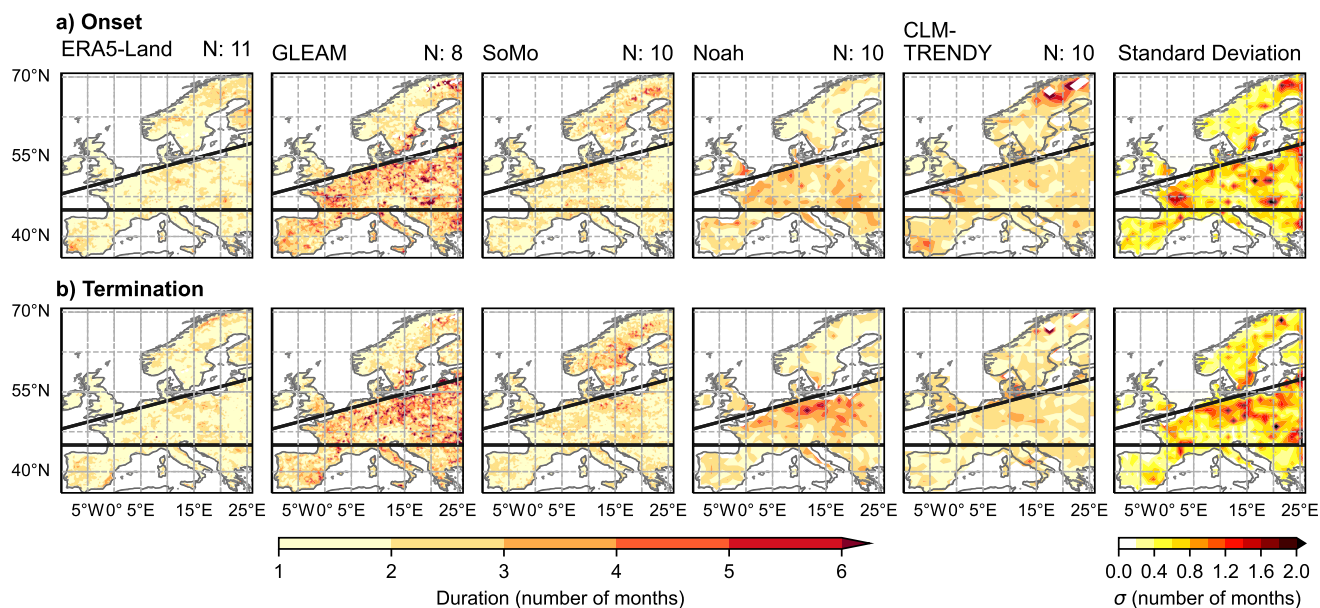


Figure 2. The mean duration of onsets and terminations of droughts over Europe during 2000–2019 for SoMo, and during 2000–2020 for the other four datasets. N indicates the median of the number of drought events over the study region. The standard deviations of the mean duration across the five soil moisture datasets are shown in the right-most column. Black thick lines separate central Europe (CEU) and Mediterranean Europe (MED) following the IPCC climate reference regions (Iturbide et al., 2020).



295 Fig. 2 indicates that within the same dataset, the mean O&T duration slightly varies across the regions in Europe. When the comparison is performed between the two spatial divisions, CEU and MED, most of the datasets tend to exhibit a slightly longer mean O&T duration in CEU compared to MED. The standard deviations across the datasets (shown in the rightmost column of Fig. 2) indicate that the discrepancies in the duration are more pronounced in CEU than in MED. In general, the difference in the mean O&T duration seems to be larger between the datasets than between the regions. It is noticeable that
 300 ERA5-Land shows shorter and GLEAM shows longer O&T duration than others. Moreover, the datasets that present longer onsets also exhibit longer terminations, implying that the duration of onsets and terminations is related across the datasets.

To illustrate better the typical O&T duration in CEU and MED, the durations of all individual events are collected from the grid points in CEU and MED from Fig. 2 and presented in the box plots in Fig. 3a and b. For ERA5-Land, GLEAM, and CLM-TRENDY, the values for the entire period 1980–2020 are also included. The averaged O&T duration over the entire CEU
 305 and MED are shown in Table 2.

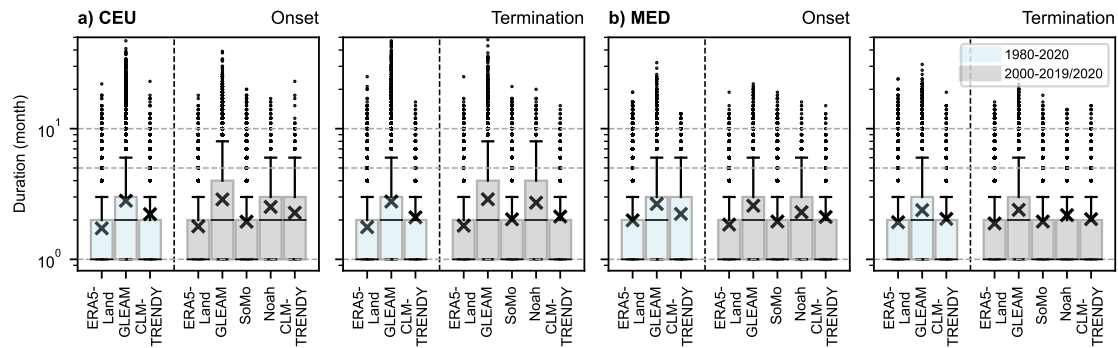


Figure 3. Duration of O&T of all individual events collected from the grid points over a) CEU and b) MED in Fig. 2 for each dataset. Black horizontal lines on the boxes indicate the medians and the crosses indicate the means of the duration. Note that the y-axis is on a logarithmic scale. Dashed grey horizontal lines indicate the duration of 1, 5, and 10 months.

Comparing the long (1980–2020) and short (2000–2020) time series, the mean O&T duration between both periods are similar in each ERA5-Land, GLEAM, and CLM-TRENDY (Fig. 3 and Table 2). Considering the period 2000–2019/2020, ERA5-Land shows the shortest mean O&T duration in both regions, with the mean values over CEU and MED ranging from 1.79 to 1.88 months (Table 2), followed by SoMo (1.94 to 2.02 months) and CLM-TRENDY (2.03 to 2.27 months). GLEAM
 310 exhibits the longest O&T duration, from 2.39 to 2.88 months. In general, the 75th percentile values of the datasets range from 2 to 4 months.

The duration between O&T within the same dataset is generally related. The datasets with short onset also exhibit short termination. Statistically, GLEAM (both periods, 1980–2020 and 2000–2020), ERA5-Land (2000–2020), and CLM-TRENDY (both periods) in CEU, SoMo, Noah, and CLM-TRENDY (2000–2020) in MED indicate that the O&T duration is the same
 315 (Table 2). Although the O&T duration for the rest is statistically different based on the t-tests, the magnitudes of O&T duration within the same dataset are relatively similar compared to the difference in the O&T duration between the datasets. The



Table 2. Mean duration of O&T (in number of months) from Fig. 3a and b. When the duration of onsets and terminations within the same dataset and region are statistically different from each other based on the t-tests at a 95% confidence level, the values are denoted with *.

		1980-2020		2000-2019	2000-2020				
		ERA5-Land	GLEAM	CLM-TRENDY	SoMo	ERA5-Land	GLEAM	Noah	CLM-TRENDY
CEU	Onset	1.73*	2.81	2.22	1.94*	1.79	2.88	2.52*	2.27
	Termination	1.76*	2.77	2.09	2.02*	1.88	2.88	2.71*	2.12
MED	Onset	1.99*	2.65*	2.23*	1.95	1.84*	2.57*	2.30	2.11
	Termination	1.92*	2.38*	2.04*	1.95	1.88*	2.39*	2.19	2.03

result implies no noticeable differences in the time required to progress into droughts and recover from droughts. Still, larger discrepancies exist in the duration of either onsets or terminations between the datasets. As presented in Figs. 2 and 3, all datasets exhibit different values for the duration, with GLEAM presenting the longest duration for both O&T.

320 Regarding the preferred seasons for O&T, the ratios of the number of onsets for each season to the total number of onsets during the 1980–2020 period, as defined in Section 3.3, are presented for ERA5-Land, GLEAM, and CLM-TRENDY in Fig. 4, and for terminations in Fig. 5. Similar to the duration, Fig. 4 and Fig. 5 show that there are regional differences within Europe regarding the occurrence timing of O&T. The majority of areas in CEU indicate JJA as the most frequent season for onsets, although not uniformly over the region and with some inconsistency in the ratios among the datasets (Fig. 4). GLEAM exhibits
 325 higher ratios distributed across extensive areas in CEU than ERA5-Land and CLM-TRENDY during JJA. Southern CEU, mainly ALP, shows higher occurrence ratios during SON in ERA5-Land and GLEAM, and during DJF in CLM-TRENDY. Over IP, onsets tend to occur more frequently during SON and DJF for all three datasets, whereas in the EMED, over Italy and the Balkans, they are most likely to occur in SON. Over Sardinia, Corsica, and northern Italy, onsets also occur during DJF in a more pronounced manner in CLM-TRENDY, but this is not evident in GLEAM.

330 For terminations (Fig. 5), more areas in CEU experience terminations during DJF and MAM. ECEU also exhibits a high frequency of terminations during SON. However, the occurrence ratios during terminations show more differences across the datasets than during onsets. For instance, ERA5-Land also exhibits a higher occurrence ratio for termination (> 0.3) in MCEU during MAM. However, this is not as apparent over the same region in GLEAM and CLM-TRENDY. This difference between the datasets also happens in MED. Over MED, higher occurrence ratios for terminations are observable during MAM in ERA5-
 335 Land and CLM-TRENDY, but this is not visible in GLEAM. In general, over IP, drought terminations occur frequently during DJF, MAM, and JJA. The majority of areas in EMED experience terminations during DJF and MAM. In general, most regions in MED agree on a relatively low occurrence of terminations during SON.

Fig. 6 summarizes the frequencies of onsets and terminations seen in Figs. 4 and 5 for each subregion by showing the median of the distribution of ratios across each domain. For onsets, Fig. 6a implies that although more subregions are considered, the
 340 seasonality of onsets over the study region can be largely divided into two spatial domains: CEU and MED. Over CEU (FR, MCEU, ALP, and ECEU), JJA is the most likely season for onsets in ERA5-Land and GLEAM, and SON in CLM-TRENDY.

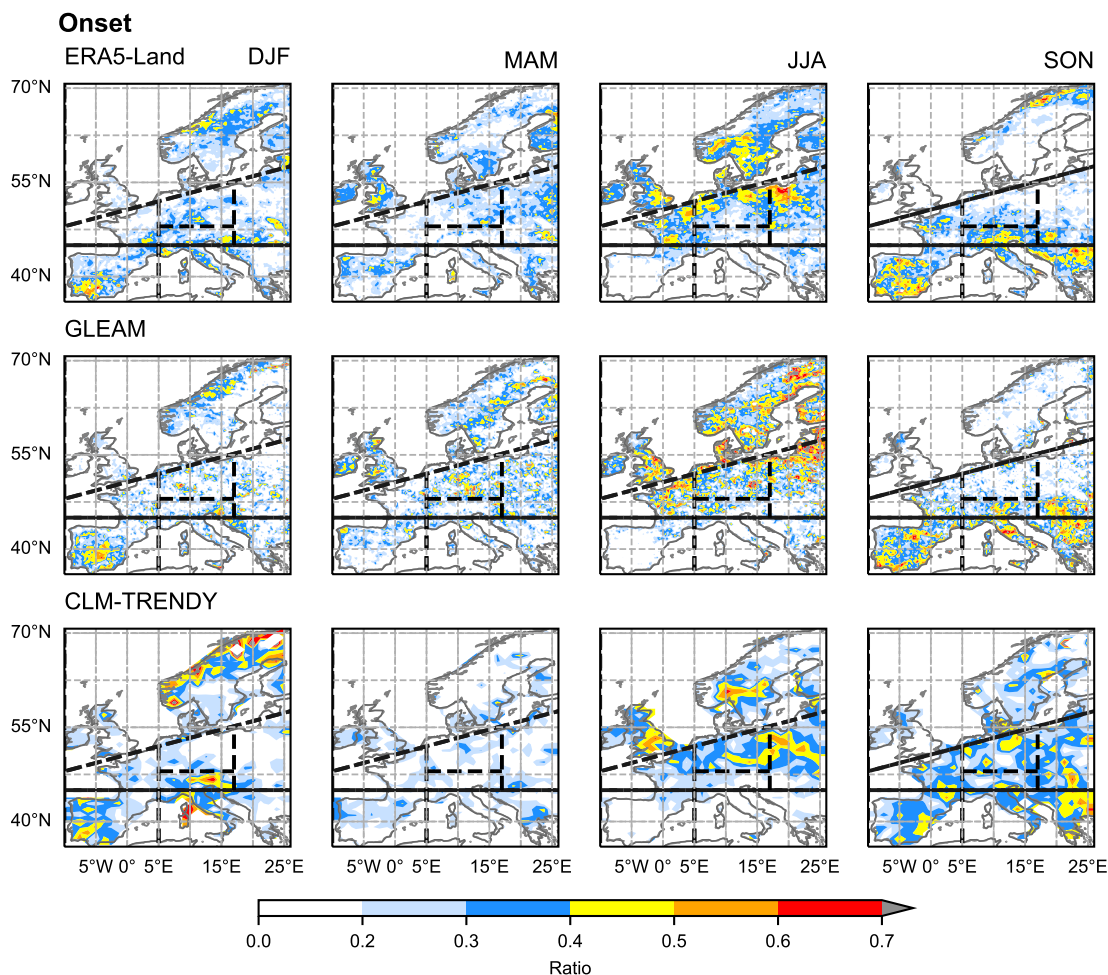


Figure 4. Ratios between the number of onsets (last month of onsets) for each season and the total number of onsets during 1980–2020 defined in Section 3.3. Black lines separate the continent into the subregions: Iberian Peninsula (IP), eastern Southern Europe (EMED), Alps (ALP), France (FR), mid-Europe (MCEU), and east central Europe (ECEU).

The most unlikely seasons range between DJF and MAM, varying across the regions and datasets. For MED (IP and EMED), all datasets unanimously indicate that the most likely season onsets is SON, followed by DJF. The least likely season for onsets is JJA.

345 The occurrence ratios of terminations do not present a robust spatial division between the two regions as onsets, and there are some discrepancies among the datasets on the seasonality of the occurrence (Fig. 6b). In CEU, over MCEU, ALP, and ECEU, GLEAM and CLM-TRENDY indicate DJF as the most likely season for terminations. For FR, GLEAM still denotes DJF, but CLM-TRENDY points to MAM as the most likely season. Nevertheless, DJF is the second most likely season in CLM-TRENDY, and the difference in the occurrence ratio between DJF and MAM is small (< 0.01). In ERA5-Land, MAM is

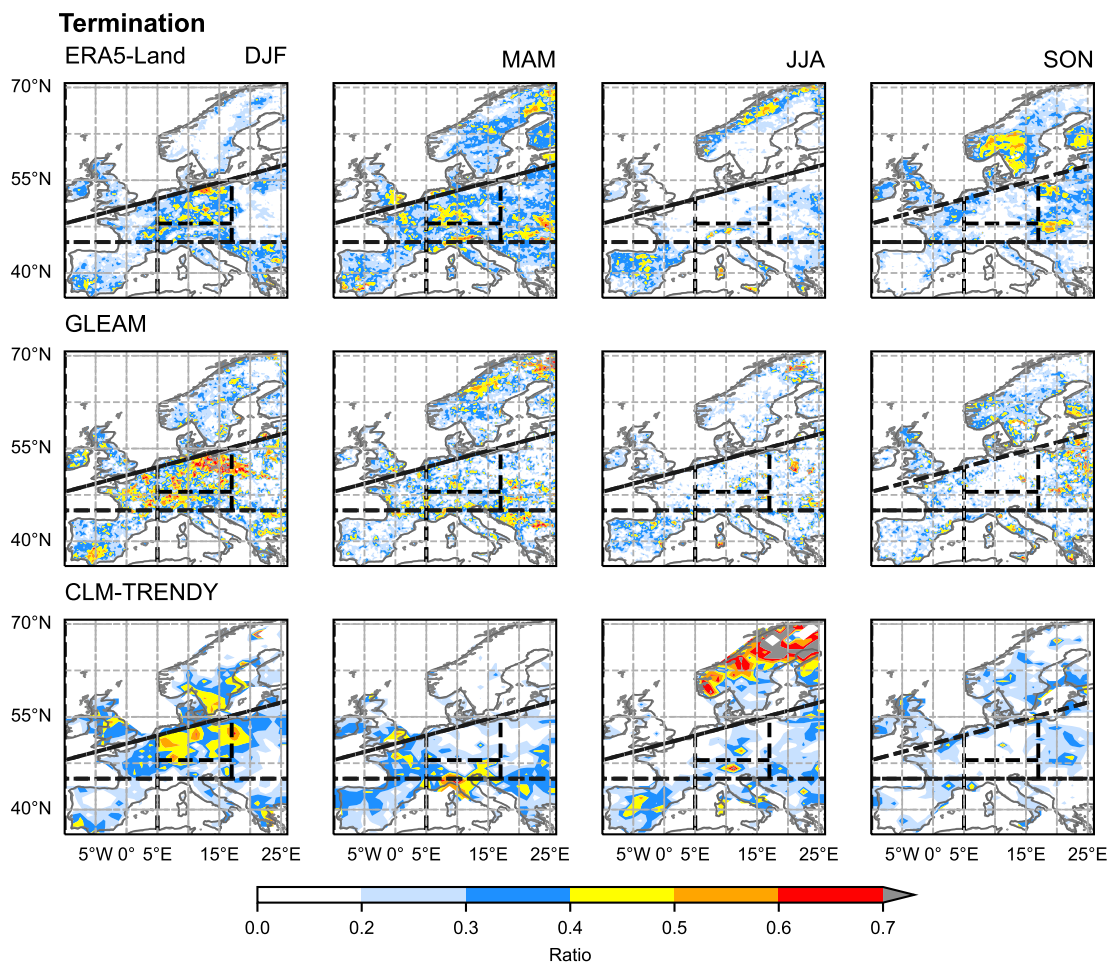


Figure 5. Same as 5, but for terminations (first month of terminations).

350 the most likely season for terminations in all regions of CEU. In FR, MCEU, and ALP, DJF is the second most likely season. In MED, over EMED, all datasets point out MAM as the most likely season for terminations. In IP, the discrepancy between the datasets for the preferred seasons for terminations is more pronounced. ERA5-Land exhibits JJA (followed closely by MAM), GLEAM presents DJF (followed by JJA), and CLM-TRENDY shows both MAM and JJA as preferred seasons for terminations.

355 In general, the preferred seasons for onsets coincide with each region's wet seasons. For CEU (FR, MCEU, ALP, and ECEU), these periods are JJA, and for MED (IP and EMED), these seasons correspond to SON and DJF, as indicated by their annual cycles, shown in Fig. 7. On the other hand, terminations tend to occur more frequently during the non-wet seasons, which are DJF and MAM in CEU, and MAM and JJA in MED. This result highlights the crucial role of precipitation availability and

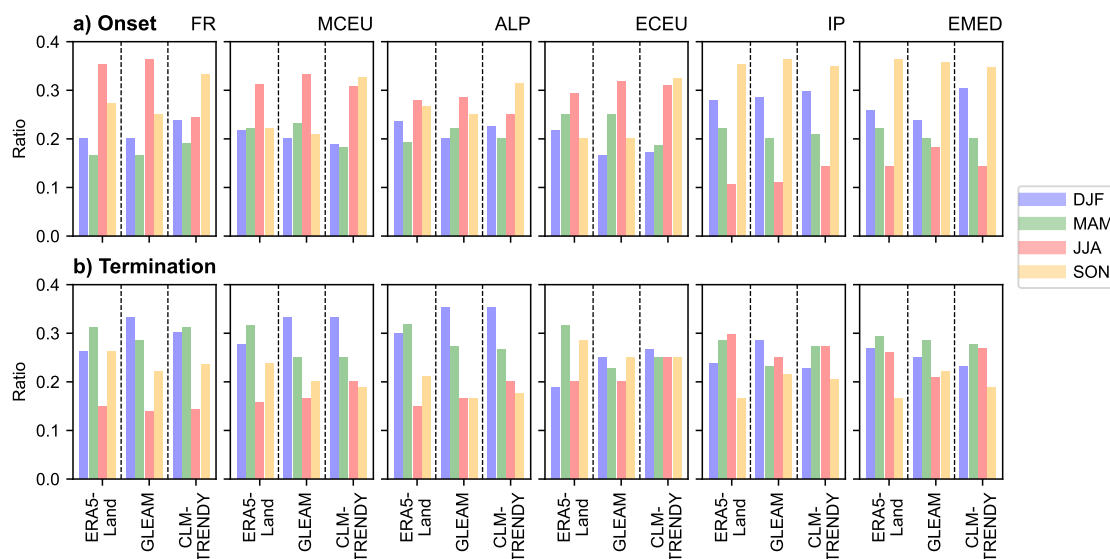


Figure 6. a) The medians of occurrence ratio of onsets for each season over all grid points in each domain from Fig. 4. (b) is the same as (a) but for terminations.

related circulations during the wet seasons in initiating dry conditions leading to drought onsets, while drought terminations are not particularly attached to the wet seasons.

Nevertheless, it is important to remark that while there are some preferred seasons for O&T showing higher occurrence ratios, O&T can still occur in other seasons, as seen in Fig. 6. The occurrence ratio of the most likely seasons does not overly exceed the ratio during other seasons. For example, in IP for ERA5-Land, the ratio for SON is 0.35, while for DJF is 0.28. The occurrence ratios for O&T are approximately 0.2 for the majority of the seasons and datasets, except during JJA in IP.

4.2 Differences in soil moisture, precipitation, and evapotranspiration among the datasets

To examine the potential origin of the differences in the duration and the preferred seasons for O&T among the datasets, we perform a comparison between the time series of ΔSM and the means of precipitation (P) and evapotranspiration (E) across the LSMs. As seen before, there are, in general, two spatial separations in the duration and seasonality of O&T (Figs. 2 and 6), CEU and MED. Thus, the study region is divided into these two to generate the time series. The time series of ΔSM for each dataset are presented in Fig. 8.

The difference in the ΔSM over time among the datasets appears to be more pronounced in CEU than MED, which is consistent with the standard deviations presented in Fig. 2. A noticeable difference is observed between GLEAM and the other two datasets before 1991. During this period, GLEAM constantly exhibits positive mean ΔSM over CEU. Regarding the dry condition since 2016, GLEAM and CLM-TRENDY present constant negative ΔSM , while ERA5-Land shows some months with positive ΔSM . The difference among the datasets is smaller in MED than in CEU, with smaller σ .

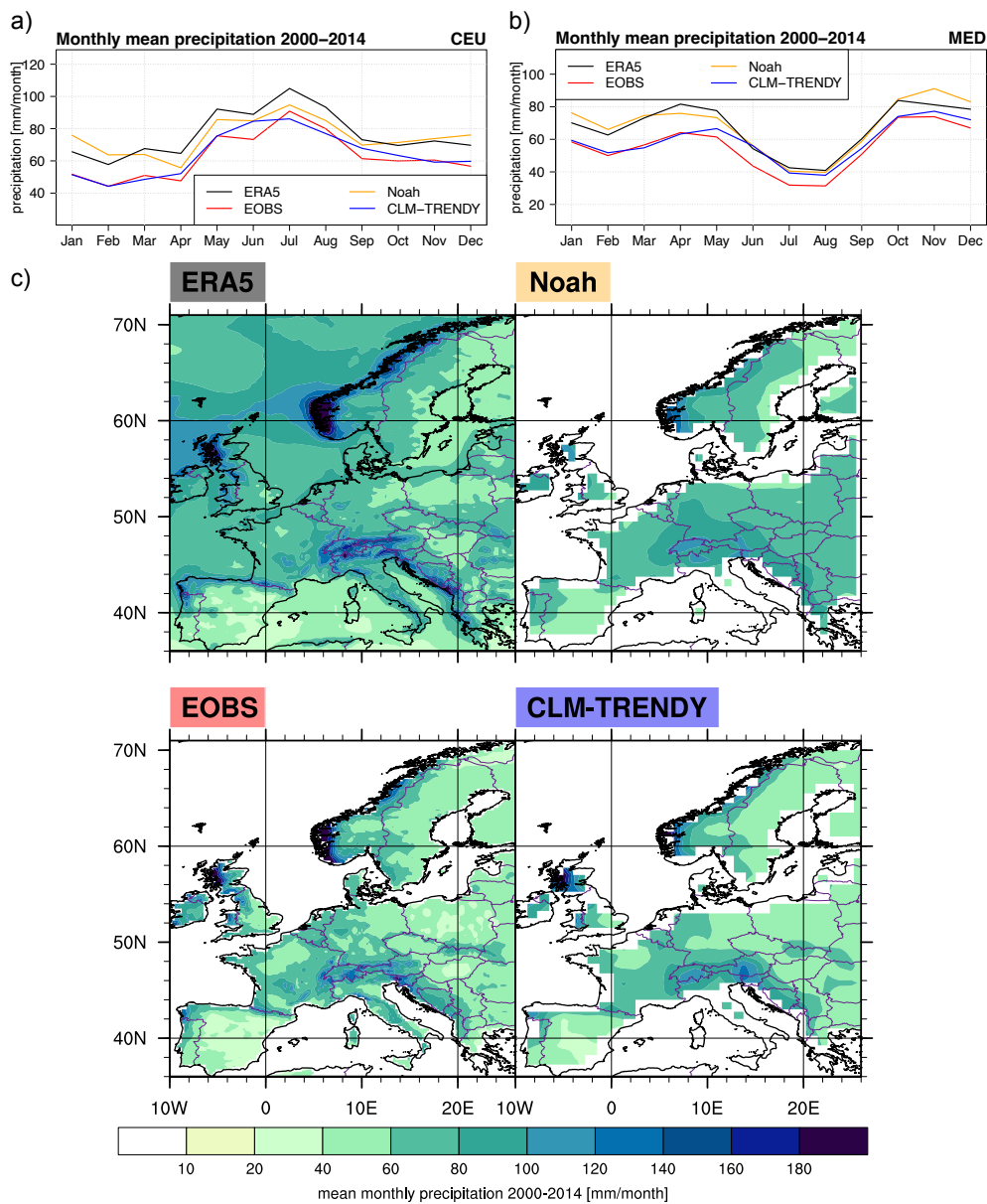


Figure 7. Annual cycles of precipitation during the reference period 2000–2014 from ERA5, Noah forcing, E-OBS, and CLM-TRENDY forcing for a) CEU and b) MED. (c) Annual mean precipitation during the same period over Europe.

E is a variable involved in the terrestrial water balance and is internally estimated by the LSMs, although it is influenced by aspects of the observational forcing as well, such as near-surface specific humidity and wind speed. Hence, the difference in E between the datasets is most likely indicative of a difference in the model’s internal physics. Evapotranspiration during 2000–2020 is shown for each of the datasets in Fig. 9.

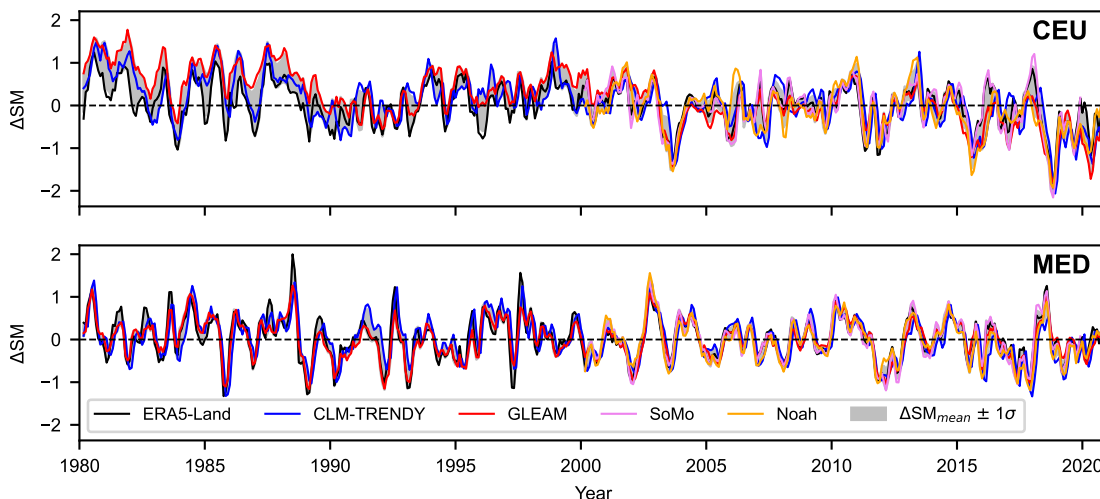


Figure 8. Spatially-weighted time series of ΔSM over CEU and MED. Grey shading denotes $\Delta SM_{mean} \pm 1\sigma$. ΔSM_{mean} is the average and σ is the standard deviation of ΔSM across the five datasets.

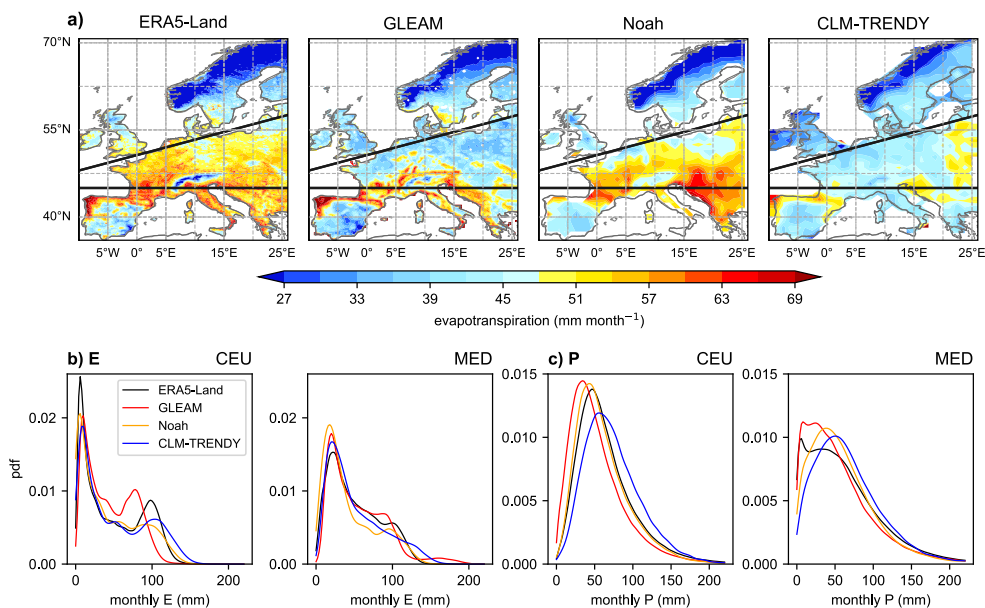


Figure 9. a) Monthly mean evapotranspiration (E) over 2000–2020 in Europe, b) probability density distributions of monthly mean evapotranspiration, and c) mean precipitation (P) over CEU and MED for the same period. SoMo is excluded as it does not contain the evapotranspiration variable.



380 Similar to the duration and preferred seasons, E varies across the regions within Europe and it also varies across datasets. In terms of the datasets, ERA5-Land and Noah exhibit higher mean E than others. GLEAM has higher values over southern CEU and northern IP. CLM-TRENDY tends to show reduced mean E compared to other datasets. GLEAM presents a longer duration of O&T than other datasets (Fig. 2 and Table 2), which can be related to reduced mean evapotranspiration due to relatively longer dry periods. In the case of CLM-TRENDY, reduced E can be caused by relatively reduced mean P compared to other datasets (Fig. 9c), primarily over CEU.

For P (Fig. 7c), which is the input forcing for LSMs, some regional differences exist among the datasets, with the largest differences over the alpine region. Nevertheless, the four datasets, in general, present consistent spatial patterns of total mean precipitation. The differences in the means are not as remarkable as evaporation, as shown in Fig. 9a. Over MED, the probability density distributions of P (Fig. 9c) indicate that some differences exist in the density distributions among the datasets, including the maximum peak of precipitation. Over CEU, CLM-TRENDY shows the P distribution shifted toward a higher mean.

Overall, the comparison of ΔSM , E, and P among the datasets suggests that varying temporal variability of ΔSM , mean E, and P contribute to the observed discrepancies in the duration and seasons among the datasets. In summary, both the models' internal physics and the ingested atmospheric forcing, i.e., P, are the contributing factors (Fang et al., 2016). Note that other variables involved in soil water balance could have been considered for the analysis, but only evapotranspiration was chosen since it is the variable available in all four soil moisture products. Obviously, there are other variables involved in soil water balance not shown here, such as surface runoff.

In spite of these differences, some similarity in the temporal variability in ΔSM is observed (Fig. 8), and the time series are significantly correlated to each other (not shown). This indicates a certain range of similarity in temporal variability exists between the datasets, inducing similar preferred seasons of occurrence.

400 **4.3 Relationship between the duration of onsets and terminations, drought intensities, precipitation, and evapotranspiration**

Next, we want to address whether the drought duration is related to the O&T duration. Do long (short) droughts also have long (short) onsets and/or terminations? The overall relationships between the duration of drought phases are presented in Fig. 10. For this, all the drought durations that correspond to a certain value of onset and termination duration are collected from all grid points over the study domain and then averaged, taking into account the spatial weights following eq. 1.

Fig. 10a and b indicate that the duration of O&T and droughts do not present a robust relationship. Longer (shorter) droughts do not necessarily have longer (shorter) O&T. Only CLM-TRENDY indicates that the drought duration is statistically significant and positively related to the onset duration, with a month of onset leading to an increase of 0.28 months in the drought duration. GLEAM exhibits a significant relationship in the duration between droughts and terminations, with an increase of 0.30 drought months every month of termination. In general, there are no unanimous directions, which means the same signs, of relationship among datasets. This result suggests that the onset duration is not indicative of the longevity of droughts, and the drought duration does not affect the termination duration.

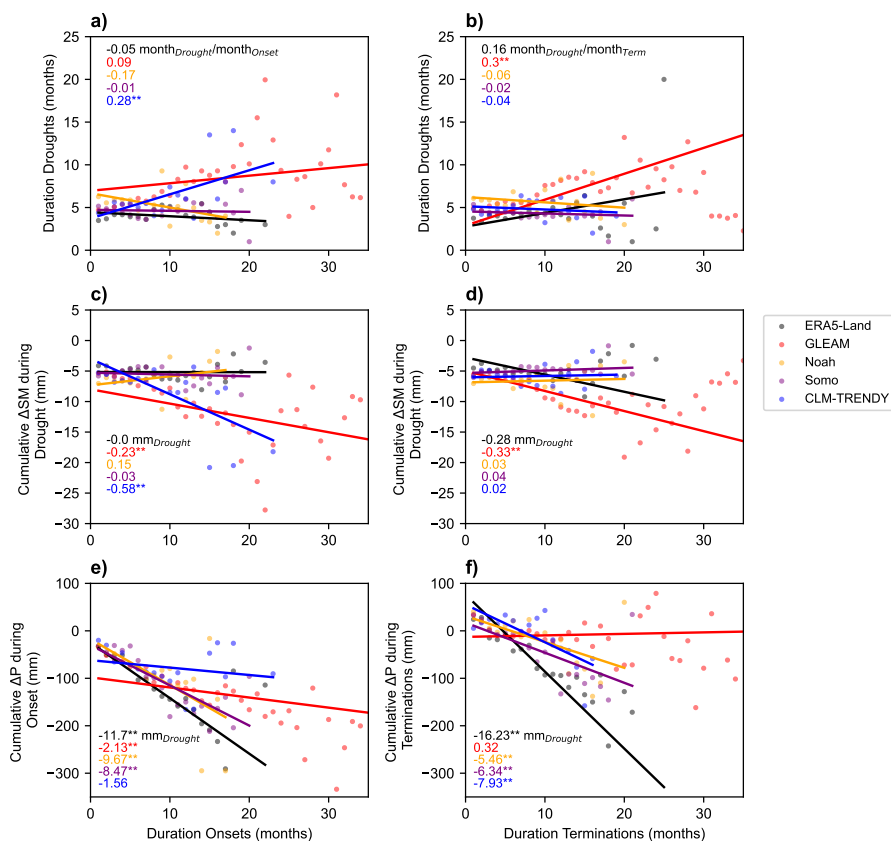


Figure 10. Relationships between (a) the mean duration of onsets and droughts, b) between the mean duration of terminations and droughts. c) and d) Same as (a) and (b) but between mean duration of O&T and drought intensities expressed in cumulative soil moisture anomalies. e) The mean duration of onsets and cumulative ΔP during the onsets, and f) the mean duration of terminations and cumulative ΔP during the terminations. The mean duration of droughts and cumulative ΔP are calculated following Section 3.4. Thick solid lines indicate the coefficients from the linear regression models between the two variables. The numbers indicate the regression coefficients denoting the degree of the relationship. When the estimated coefficients are statistically different from zero at a 95% confidence level based on the Wald test, the values are denoted with **.

The same finding is observed in terms of intensities of droughts (Fig. 10c and d). Intensities of droughts, represented as cumulative ΔSM during droughts (more negative cumulative ΔSM , more intense the drought), and the duration of either onsets or terminations do not consistently show statistically significant relationships in all datasets. Only GLEAM and CLM-TRENDY exhibit statistically significant relationships, indicating decreases of 0.23 mm and 0.58 mm in soil moisture every month of onset, respectively. For terminations, GLEAM is the only dataset showing that intense droughts have longer termination (a decrease in 0.33 mm of soil moisture linked with a month of termination).



How ΔP progressing during onsets and terminations are linked to the O&T duration is also examined (Fig. 10e and f). This analysis is to evaluate whether the magnitude of changes in ΔP can signal a drought initiation or a potential drought termination and, consequently, an early warning based on this relationship. For onsets, all datasets indicate negative relationships between the onset duration and the cumulative ΔP ; among them, four datasets (ERA5-Land, GLEAM, Noah, and CLM-TRENDY) denote statistically significant relationships. The duration of terminations also presents negative relationships to the cumulative ΔP , with four datasets (ERA5-Land, Noah, SoMo, and CLM-TRENDY) exhibiting statistically significant values. Longer terminations mean more periods in dry conditions where cumulative negative ΔP increases. Hence, a longer termination does not necessarily mean more periods of precipitation that lead to the end of droughts. A similar result is observed when instead of cumulative ΔP , cumulative $\Delta(P-E)$ is analyzed (Fig. S3 in the supplement), meaning that the magnitude of ΔP (or $\Delta(P-E)$) gives a prior indication of the duration of O&T.

Overall, the result indicates that the duration and intensities of droughts do not give a specific indication of the duration of onsets and terminations. On the other hand, in terms of the water balance conditions, ΔP and (or $\Delta(P-E)$) become more negative with longer onsets and terminations. This means that ΔP can potentially offer an early signal regarding the potential duration of drought onsets and terminations, given its magnitudes.

4.4 Atmospheric circulations associated with onsets and terminations

To understand the atmospheric circulation involved in each drought phase and which circulation conditions help onsets to progress into droughts, the mean circulation patterns during onsets, terminations, and no drought dry periods (NDDs) are examined and are presented in Fig. 11.

In all onsets, the mean circulation patterns (Fig. 11a) are characterized by an anticyclonic circulation and negative ΔP over the regions where droughts take place. Although the exact location of the system slightly differs, large-scale anticyclonic pressure systems in Europe during onsets resemble the circulation patterns that were observed during the recent European droughts (Ionita et al., 2017; García-Herrera et al., 2019) and the pattern associated with a strong reduction in precipitation over the region affected by droughts (Gessner et al., 2022). This system can further decrease precipitation by inhibiting the incoming moisture from the Mediterranean Sea and the Atlantic Ocean since it is associated with weakened westerlies.

During NDDs (Fig. 11b), similar anticyclonic patterns occur over extensive areas in Europe, also with negative ΔP . However, we found that the magnitude of ΔGP over the affected region is lower during NDDs than those of onsets. In addition, the occurrence of positive ΔGP is less frequent during NDDs, indicating that the persistence of the anticyclonic system is required to make dry conditions progress into droughts.

During terminations (Fig. 11c), ECEU and EMED show a cyclonic pattern over northern Europe. For other regions, the mean circulation patterns do not show well-defined structures over the region where termination takes place, unlike onsets, implying that opposite cyclonic conditions over the affected regions are not strictly required for terminations. Instead, a high-pressure system located over the North Atlantic Ocean is observed during terminations in all regions except in ECEU. Anticyclonic circulation associated with this pressure system in the North Atlantic can bring moisture from the higher latitudes to the continent. Terminations occurring in MED (IP and EMED) show positive ΔGP in the southern regions (about below 45°) and

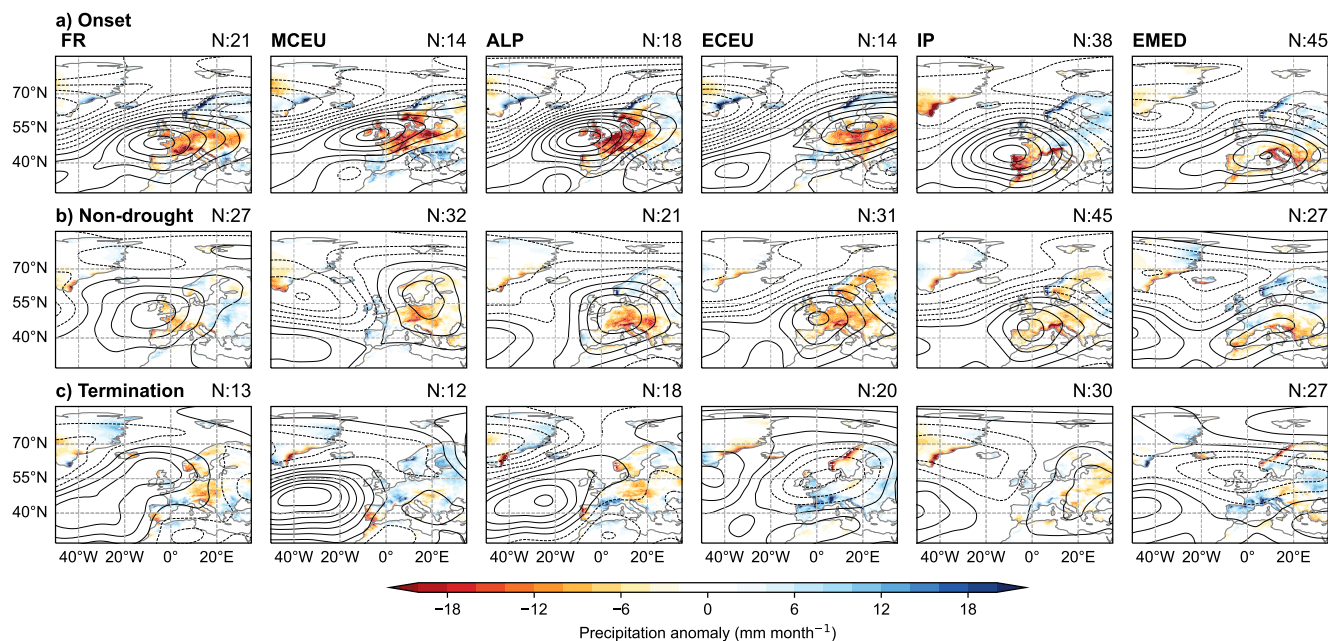


Figure 11. a) Mean geopotential height anomalies at 500 hPa (ΔGP) during drought onsets (in contour lines every 6 gpm, where the dotted lines denote negative anomalies) and ΔP (color-shaded) associated with considered onsets for each of the subregions, b) and c) Same as (a) but averaged over that season in no-drought dry periods and terminations, respectively, following Section 3.5. Drought phases for a-c are defined using the spatially weighted averaged time series of ΔSM for each subregion. N indicates the number of timesteps considered for the composites.

negative ΔGP in the north. In general, a weakened ΔGP is observed over each region of interest, and positive ΔP is evident during the termination phase.

455 Similar results of anticyclonic circulation during onsets and NDDs and weakened ΔGP during terminations are also found for seasonal analysis. A slight difference is observed in the location of the anticyclonic patterns during onsets and NDDs depending on the season (Figs. S4 to S6).

To assess the overall relationship between drought phases and NAO, the correlation between the NAO index and monthly or seasonally averaged soil moisture anomalies is presented in Fig. 12a and b. Fig. 12a indicates that when considering all months, 460 NAO is negatively correlated with soil moisture over CEU and MED, suggesting a positive NAO associated with a decrease in soil moisture over CEU and MED. Although it is not within the regions of our interest, soil moisture in the Scandinavian region is positively correlated to NAO. These relationships between soil moisture and NAO agree with Almendra-Martín et al. (2022), who showed a dominant influence of the NAO on soil moisture variability in Europe. However, the correlation coefficients vary with seasons. During JJA, the positive correlation coefficients dominate over a large portion of MED, and 465 during SON in southeastern IP. The correlation coefficients are positive during DJF over MCEU and ECEU. The result suggests a varying influence of NAO on soil moisture droughts depending on the season. In general, over MED, the effect of NAO on



soil moisture droughts is strong during DJF and MAM, and also during SON over EMED, with negative correlations. The correlations become weaker during JJA. For CEU, the correlations are negative during MAM and JJA. EMED shows more negative correlations during SON. The correlations become positive during DJF in MCEU, indicating less influence of NAO on soil moisture droughts in the region, while the correlations are negative in FR. These seasons seem to be consistent with the preferred seasons for onsets and terminations of each region shown in Fig. 6. It is noticeable that the Alpine region exhibits a clear opposite correlation pattern to the rest of the regions, which emphasizes the complex topography of this area.

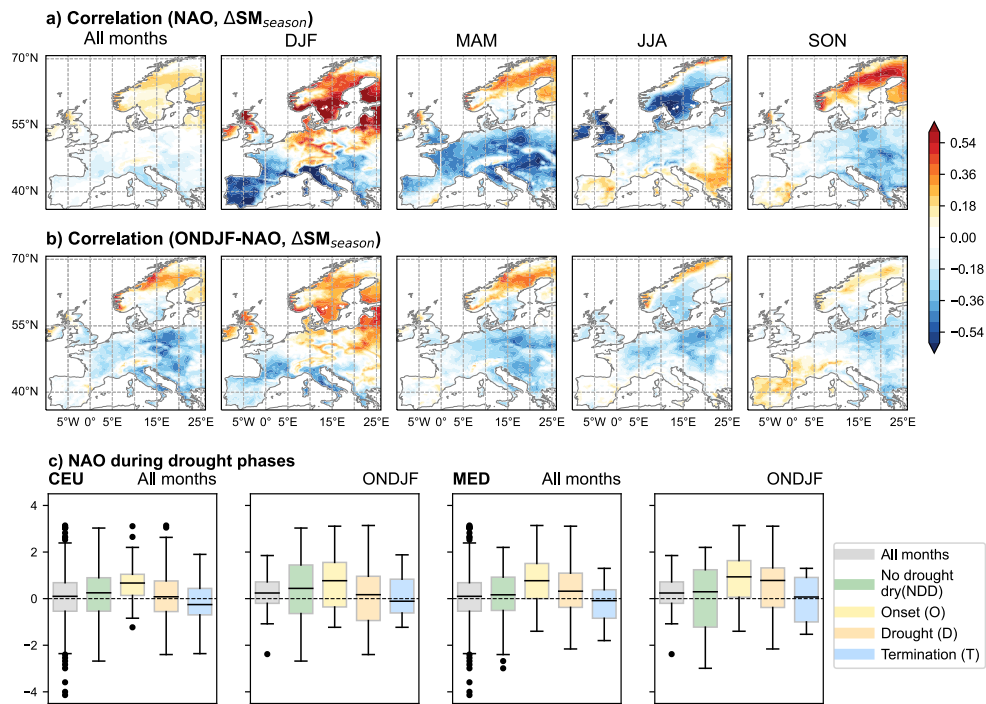


Figure 12. a) Pearson correlation coefficients between the NAO index and monthly or seasonally averaged soil moisture anomalies (ΔSM_{season}) for all periods and each season, and b) between the cold-season (October-February) NAO indices and ΔSM_{season} for each season. c) NAO index values during each drought phase and NDD. The medians are marked in black lines. Drought phases are estimated using the spatially-weighted time series of ΔSM in Fig. 8.

Knowing that the strength of NAO increases during the cold seasons, the correlation coefficients are also calculated between the mean October-February NAO index and soil moisture anomalies, which is shown in Fig. 12b. In all seasons, the correlation patterns are similar to those in Fig. 12a. The difference is that during DJF, the positive correlations are extended toward ECEU and Balkan regions. During MAM and JJA, the magnitudes of coefficients are reduced over MED. During SON, positive coefficients are expanded to northern IP and FR.

To focus on the influence of NAO during each drought phase, the monthly and ONDJF NAO values are separated into drought phases and NDDs in CEU and MED and presented in the box plot in Fig. 12c. The mean NAO values for each phase



480 are shown in Table 3. For both the monthly and the cold-season NAO, positive NAO tends to occur more frequently during onsets than other phases. Persistent anticyclonic circulation observed during onsets in Fig. 11a can be associated with more frequent positive NAO, which leads to a weakening of westerlies as a moisture source from the Atlantic. In MED, positive NAO occurs more frequently during onsets and also during droughts.

In terms of the statistical difference in the mean values of NAO between the drought phases (Table 3), for MED, the mean NAO during onsets differs statistically from the mean NAO during the other phases. The result indicates that positive NAO occurs more frequently during onsets than other phases. The same result is obtained with the cold-season NAO during all drought phases, except for droughts. In the case of CEU, the difference between the mean NAO during onsets and other phases is statistically not pronounced when considering the cold-season NAO. However, considering all monthly NAO, the means are statistically different between onsets and all phases except for NDD.

490 Despite no statistical difference in some phases, it is clear that the mean NAOs are more positive during onsets than other phases in both regions. The differences in the mean values of NAO between onsets and NDDs are large (0.38 to 0.82), suggesting that persistent anticyclonic during onsets could be related to the frequent positive NAO. Terminations show more neutral or slight negative NAO, implying that a negative NAO condition is not strictly necessary to terminate droughts. Overall, the result shows that positive NAO occurs more frequently during the initial dry conditions preceding droughts, implying the role of NAO as an early warning of droughts.

Table 3. Mean NAO index values from Fig. 12c. When the mean NAO is statistically different from those during onsets based on the t-tests at 95% confidence level, the values are denoted with *.

		All	Onset	Drought	No drought dry	Termination
CEU	All months	0.10*	0.65	0.15*	0.27	-0.07*
	ONDJF	0.19	0.76	0.14	0.37	0.15
MED	All months	0.10*	0.79	0.35*	0.07*	-0.17*
	ONDJF	0.20*	0.83	0.52	0.01*	-0.11*

5 Discussions and conclusion

We have examined temporal characteristics, namely the typical duration and the seasons of occurrence, and atmospheric circulation associated with drought onsets and terminations (O&T) in central (CEU) and Mediterranean Europe (MED) from 1980 to 2020. Soil moisture droughts are quantified using the upper 10 cm soil moisture anomalies from five different soil moisture datasets: ERA5-Land, GLEAM, SoMo, Noah, and CLM-TRENDY. The drought life cycle is divided into three phases: onset, drought, and termination. Onsets and terminations are the transition periods to droughts and from droughts to normal conditions, respectively. This means that onsets are defined as the dry periods preceding the drought threshold, while terminations are the periods from the drought threshold to the neutral conditions.



We found that there are some differences in the duration of O&T across Europe and among the five soil moisture datasets used in this study. In general, CEU tends to exhibit a longer duration for both O&T compared to those over MED. In terms of the datasets, while ERA5-Land shows a shorter O&T duration in all phases, GLEAM exhibits a longer duration than other datasets. However, within the same datasets, the difference between O&T duration is relatively small, and for some datasets and periods, without any statistical difference. This suggests that the range of durations of onsets and terminations are similar.

Regarding the seasons of occurrence of O&T, the wet seasons are the most likely periods for onsets in CEU and MED. These are summer (JJA) for CEU and autumn (SON) and winter (DJF) for MED. This emphasizes the importance of precipitation availability and related atmospheric circulation during the wet seasons in initiating droughts. For terminations, there are no consistent seasons of occurrence among the datasets, but in general, the most likely periods for terminations occur during non-wet seasons. Nevertheless, although there are some preferred seasons for onsets, they can still take place in other seasons, and the frequency of occurrence during the most likely seasons does not overly exceed the frequency during other seasons.

The observed discrepancies in the duration and seasonality of O&T among the datasets seem to be partially explained by LSM's internal physics and input atmospheric forcings (Fang et al., 2016). This discrepancy needs to be considered when drought studies are based on a single soil moisture dataset. Still, the existence of some common seasons of occurrence of drought phases implies a certain range of similarity in the temporal variability of soil moisture across different LSMs.

By linking precipitation anomalies and the O&T duration, we found that the magnitudes of cumulative precipitation deficits are straightforwardly related to the duration of onsets or termination. Hence, the variable can serve as a direct indication of potential O&T duration.

In terms of atmospheric circulation anomalies, drought onsets are associated with anticyclonic atmospheric circulation patterns, a finding that agrees with Lhotka et al. (2020). For terminations, there are not unanimous patterns that different subregions in Europe share in common. In general, terminations are linked with circulation patterns with reduced magnitudes without a well-defined structure over the region where droughts occur. Terminations occurring over eastern Central Europe and the eastern Mediterranean, cyclonic circulation that occupies central and northern Europe is observed. Circulation patterns during onsets are stronger and more persistent than those during the normal light dry periods.

In addition, during onsets, the mean NAO is positive, indicating more frequent positive NAO than during other drought phases. The mean NAO during onsets is statistically higher than in other drought phases, including droughts, and the effects of NAO are more pronounced in MED than CEU. This indicates the important role of this large-scale circulation pattern during onsets in initiating a reduction of moisture supply and persistence of anticyclonic patterns during the most likely seasons of drought onsets. The finding remarks on the potential usage of the NAO index during onsets as an early warning for droughts. The mean NAO during terminations is in a neutral state.

Our study is one of the few that have investigated the onset and termination of droughts in Europe on a pan-continental scale over central and Mediterranean regions, providing clear, distinct temporal and circulation characteristics involved in different drought phases. A downside of this study would be that the temporal extent of the datasets, 20 to 40 years, may not be long enough to capture all possible variability of drought onsets and terminations.



It is also important to remark that regional differences in the temporal characteristics of onset and termination are observed within CEU and MED. Europe is characterized by complex topography and is located in the transition zone from a semi-arid
540 climate in the south to a relatively temperate wet climate in the north. Therefore, each climate may present different drought characteristics, which are related also to the seasonality of precipitation. Our analysis separates regional domains considering these climate aspects by largely following Christensen and Christensen (2007). However, it may not take into account very small-scale regional differences within these domains.

More understanding of onsets and terminations is certainly necessary to improve early predictions and preparedness for
545 potentially devastating droughts. How the life cycle of droughts is influenced by anthropogenic warming would be the follow-up research question that needs to be addressed to understand how these extreme hydrological events might change in the future.

Code availability. The python script with a function for drought phases estimation is available on the corresponding author's GitHub https://github.com/wmk21/drought_estimation.

550 *Data availability.* The datasets used in this study are available online in: ERA5 and ERA5-Land at <https://cds.climate.copernicus.eu/>, GLDAS LSMs at <https://ldas.gsfc.nasa.gov/gldas>, GLEAM at <https://www.gleam.eu/>, E-OBS at <https://www.ecad.eu/download/ensembles/download.php>, and SoMo.ml at https://www.bgc-jena.mpg.de/geodb/BGI/somo_ml_v1.php. The monthly NAO index is obtained from <https://climatedataguide.ucar.edu/climate-data/hurrell-north-atlantic-oscillation-nao-index-station-based>.

Author contributions. WMK designed the study, performed the principal analysis, and drafted the manuscript. SJGR provided the analysis
555 of the precipitation cycles and feedback on the methodology and results. IRS provided critical feedback throughout the analysis and on the results. SJGR and IRS contributed to the interpretation of the result and writing the manuscript. DK provided the CLM-TRENDY simulation and details about it.

Competing interests. The authors declare that they have no conflict of interest.

Acknowledgements. We thank all the research groups that produced the datasets used in this study and for making their output publicly
560 available. We acknowledge the Copernicus program for the ERA5 and ERA5-Land data (Hersbach et al., 2020; Muñoz-Sabater et al., 2021) available in Copernicus Climate Change Service Climate Data Store, the NASA/NOAA Global Land Data Assimilation System for the Noah and Catchment Land Surface Model datasets (Rodell et al., 2004), <https://www.gleam.eu/> for GLEAM v3 (produced by Dr. Akash Koppa and validated by Dr. Petra Hulsman, Martens et al., 2017), ECA&D for E-OBS (Klein Tank et al., 2002; Klok and Klein Tank, 2009; Cornes



565 et al., 2018), O and Orth (2021) and Max Plank Institute for Biogeochemistry for SoMo.ml dataset, and the Climate Data guide project at NCAR for the NAO index (Schneider et al., 2013; Hurrell et al., 2023), and the Global Carbon Project (Friedlingstein et al., 2022) for the CLM-TRENDY simulation. WMK thanks Vít Svoboda (JILA, CU Boulder) for his comments on plotting and the drought estimation function. WMK acknowledges funding from the Swiss National Science Foundation (grant number P500PN_206653). This work is supported by the NSF National Center for Atmospheric Research, which is a major facility sponsored by the National Science Foundation under the Cooperative Agreement 1852977.



570 References

- Almendra-Martín, L., Martínez-Fernández, J., Piles, M., González-Zamora, , Benito-Verdugo, P., and Gaona, J.: Influence of atmospheric patterns on soil moisture dynamics in Europe, *Science of The Total Environment*, 846, <https://doi.org/10.1016/j.scitotenv.2022.157537>, 2022.
- Bachmair, S., Svensson, C., Hannaford, J., Barker, L. J., and Stahl, K.: A quantitative analysis to objectively appraise drought indicators and
575 model drought impacts, *Hydrology and Earth System Sciences*, 20, 2589–2609, <https://doi.org/10.5194/hess-20-2589-2016>, 2016.
- Christensen, J. H. and Christensen, O. B.: A summary of the PRUDENCE model projections of changes in European climate by the end of this century, *Climatic change*, 81, 7–30, <https://doi.org/https://doi.org/10.1007/s10584-006-9210-7>, 2007.
- Cook, B. I., Mankin, J. S., and Anchukaitis, K. J.: Climate change and drought: From past to future, *Current Climate Change Reports*, 4, 164–179, <https://doi.org/10.1007/s40641-018-0093-2>, 2018.
- 580 Cornes, R. C., van der Schrier, G., van den Besselaar, E. J. M., and Jones, P. D.: An Ensemble Version of the E-OBS Temperature and Precipitation Data Sets, *Journal of Geophysical Research: Atmospheres*, 123, 9391–9409, <https://doi.org/10.1029/2017JD028200>, 2018.
- Dai, A.: Drought under global warming: a review, *WIREs Climate Change*, 2, 45–65, <https://doi.org/10.1002/wcc.81>, 2011.
- Fang, L., Hain, C. R., Zhan, X., and Anderson, M. C.: An inter-comparison of soil moisture data products from satellite remote sensing and a land surface model, *International Journal of Applied Earth Observation and Geoinformation*, 48, 37–50,
585 <https://doi.org/10.1016/j.jag.2015.10.006>, 2016.
- Faranda, D., Pascale, S., and Bulut, B.: Persistent anticyclonic conditions and climate change exacerbated the exceptional 2022 European-Mediterranean drought, *Environmental Research Letters*, 18, 034 030, <https://doi.org/10.1088/1748-9326/acbc37>, 2023.
- Friedlingstein, P., O’Sullivan, M., Jones, M. W., Andrew, R. M., Gregor, L., Hauck, J., Le Quéré, C., Luijkx, I. T., Olsen, A., Peters, G. P., Peters, W., Pongratz, J., Schwingshackl, C., Sitch, S., Canadell, J. G., Ciais, P., Jackson, R. B., Alin, S. R., Alkama, R., Arneeth, A.,
590 Arora, V. K., Bates, N. R., Becker, M., Bellouin, N., Bittig, H. C., Bopp, L., Chevallier, F., Chini, L. P., Cronin, M., Evans, W., Falk, S., Feely, R. A., Gasser, T., Gehlen, M., Gkritzalis, T., Gloege, L., Grassi, G., Gruber, N., Gürses, , Harris, I., Hefner, M., Houghton, R. A., Hurtt, G. C., Iida, Y., Ilyina, T., Jain, A. K., Jersild, A., Kadono, K., Kato, E., Kennedy, D., Klein Goldewijk, K., Knauer, J., Korsbakken, J. I., Landschützer, P., Lefèvre, N., Lindsay, K., Liu, J., Liu, Z., Marland, G., Mayot, N., McGrath, M. J., Metzl, N., Monacci, N. M., Munro, D. R., Nakaoka, S.-I., Niwa, Y., O’Brien, K., Ono, T., Palmer, P. I., Pan, N., Pierrot, D., Pockock, K., Poulter, B., Resplandy, L.,
595 Robertson, E., Rödenbeck, C., Rodriguez, C., Rosan, T. M., Schwinger, J., Séférian, R., Shutler, J. D., Skjelvan, I., Steinhoff, T., Sun, Q., Sutton, A. J., Sweeney, C., Takao, S., Tanhua, T., Tans, P. P., Tian, X., Tian, H., Tilbrook, B., Tsujino, H., Tubiello, F., van der Werf, G. R., Walker, A. P., Wanninkhof, R., Whitehead, C., Willstrand Wranne, A., Wright, R., Yuan, W., Yue, C., Yue, X., Zaehle, S., Zeng, J., and Zheng, B.: Global Carbon Budget 2022, *Earth System Science Data*, 14, 4811–4900, <https://doi.org/10.5194/essd-14-4811-2022>, publisher: Copernicus GmbH, 2022.
- 600 García-Herrera, R., Garrido-Perez, J. M., Barriopedro, D., Ordóñez, C., Vicente-Serrano, S. M., Nieto, R., Gimeno, L., Sorí, R., and Yiou, P.: The European 2016/17 Drought, *Journal of Climate*, 32, 3169–3187, <https://doi.org/10.1175/JCLI-D-18-0331.1>, 2019.
- Gessner, C., Fischer, E. M., B. U., and Knutti, R.: Multi-year drought storylines for Europe and North America from an iteratively perturbed global climate model, *Weather and Climate Extremes*, 38, <https://doi.org/10.1016/j.wace.2022.100512>, 2022.
- Hari, V., Rakovec, O., Markonis, Y., Hanel, M., and Kumar, R.: Increased future occurrences of the exceptional 2018–2019 Central European
605 drought under global warming, *Scientific Reports*, 10, 12 207, <https://doi.org/10.1038/s41598-020-68872-9>, 2020.



- Hersbach, H., Bell, B., Berrisford, P., Hirahara, S., Horányi, A., Muñoz-Sabater, J., Nicolas, J., Peubey, C., Radu, R., Schepers, D., Simmons, A., Soci, C., Abdalla, S., Abellan, X., Balsamo, G., Bechtold, P., Biavati, G., Bidlot, J., Bonavita, M., De Chiara, G., Dahlgren, P., Dee, D., Diamantakis, M., Dragani, R., Flemming, J., Forbes, R., Fuentes, M., Geer, A., Haimberger, L., Healy, S., Hogan, R. J., Hólm, E., Janisková, M., Keeley, S., Laloyaux, P., Lopez, P., Lupu, C., Radnoti, G., de Rosnay, P., Rozum, I., Vamborg, F., Vil-laume, S., and Thépaut, J.-N.: The ERA5 global reanalysis, *Quarterly Journal of the Royal Meteorological Society*, 146, 1999–2049, <https://doi.org/10.1002/qj.3803>, 2020.
- 610 Hurrell, J., Phillips, A., and for Atmospheric Research Staff [eds], N. C.: The Climate Data Guide: Hurrell (2003) North Atlantic Oscillation (NAO) Index (station-based), <https://climatedataguide.ucar.edu/climate-data/hurrell-north-atlantic-oscillation-nao-index-station-based>, last access on Nov 5, 2023, 2023.
- 615 Hurrell, J. W., Kushnir, Y., Ottersen, G., and Visbeck, M.: An overview of the North Atlantic oscillation, *Geophysical Monograph-American Geophysical Union*, 134, 1–36, <https://doi.org/10.1029/134GM01>, 2003.
- Ionita, M., Tallaksen, L. M., Kingston, D. G., Stagge, J. H., Laaha, G., Van Lanen, H. A. J., Scholz, P., Chelcea, S. M., and Haslinger, K.: The European 2015 drought from a climatological perspective, *Hydrology and Earth System Sciences*, 21, 1397–1419, <https://doi.org/10.5194/hess-21-1397-2017>, 2017.
- 620 Iturbide, M., Gutiérrez, J. M., Alves, L. M., Bedia, J., Cerezo-Mota, R., Gimeno, E., Cofiño, A. S., Di Luca, A., Faria, S. H., Gorodetskaya, I. V., Hauser, M., Herrera, S., Hennessy, K., Hewitt, H. T., Jones, R. G., Krakovska, S., Manzananas, R., Martínez-Castro, D., Narisma, G. T., Nurhati, I. S., Pinto, I., Seneviratne, S. I., van den Hurk, B., and Vera, C. S.: An update of IPCC climate reference regions for subcontinental analysis of climate model data: definition and aggregated datasets, *Earth System Science Data*, 12, 2959–2970, <https://doi.org/10.5194/essd-12-2959-2020>, 2020.
- 625 Klein Tank, A. M. G., Wijngaard, J. B., Können, G. P., Böhm, R., Demarée, G., Gocheva, A., Miletta, M., Pashiardis, S., Hejkrlik, L., Kern-Hansen, C., Heino, R., Bessemoulin, P., Müller-Westermeier, G., Tzanakou, M., Szalai, S., Pálsdóttir, T., Fitzgerald, D., Rubin, S., Capaldo, M., Maugeri, M., Leitass, A., Bukantis, A., Aberfeld, R., van Engelen, A. F. V., Forland, E., Mielus, M., Coelho, F., Mares, C., Razuvaev, V., Nieplova, E., Cegnar, T., Antonio López, J., Dahlström, B., Moberg, A., Kirchhofer, W., Ceylan, A., Pachaliuk, O., Alexander, L. V., and Petrovic, P.: Daily dataset of 20th-century surface air temperature and precipitation series for the European Climate Assessment, *International Journal of Climatology: A Journal of the Royal Meteorological Society*, 22, 1441–1453, <https://doi.org/doi.org/10.1002/joc.773>, 2002.
- 630 Klok, E. J. and Klein Tank, A. M. G.: Updated and extended European dataset of daily climate observations, *International Journal of Climatology: A Journal of the Royal Meteorological Society*, 29, 1182–1191, <https://doi.org/doi.org/10.1002/joc.1779>, 2009.
- Koren, V., Schaake, J., Mitchell, K., Duan, Q.-Y., Chen, F., and Baker, J. M.: A parameterization of snowpack and frozen ground intended for NCEP weather and climate models, *Journal of Geophysical Research: Atmospheres*, 104, 19 569–19 585, <https://doi.org/10.1029/1999JD900232>, 1999.
- 635 Lawrence, D. M., Fisher, R. A., Koven, C. D., Oleson, K. W., Swenson, S. C., Bonan, G., Collier, N., Ghimire, B., van Kampenhout, L., Kennedy, D., Kluzek, E., Lawrence, P. J., Li, F., Li, H., Lombardozzi, D., Riley, W. J., Sacks, W. J., Shi, M., Vertenstein, M., Wieder, W. R., Xu, C., Ali, A. A., Badger, A. M., Bisht, G., van den Broeke, M., Brunke, M. A., Burns, S. P., Buzan, J., Clark, M., Craig, A., Dahlin, K., Drewniak, B., Fisher, J. B., Flanner, M., Fox, A. M., Gentine, P., Hoffman, F., Keppel-Aleks, G., Knox, R., Kumar, S., Lenaerts, J., Leung, L. R., Lipscomb, W. H., Lu, Y., Pandey, A., Pelletier, J. D., Perket, J., Randerson, J. T., Ricciuto, D. M., Sanderson, B. M., Slater, A., Subin, Z. M., Tang, J., Thomas, R. Q., Val Martin, M., and Zeng, X.: The Community Land Model Version 5: Description



- of New Features, Benchmarking, and Impact of Forcing Uncertainty, *Journal of Advances in Modeling Earth Systems*, 11, 4245–4287, <https://doi.org/10.1029/2018MS001583>, 2019.
- 645 Lhotka, O., Trnka, M., Kyselý, J., Markonis, Y., Balek, J., and Možný, M.: Atmospheric Circulation as a Factor Contributing to Increasing Drought Severity in Central Europe, *Journal of Geophysical Research: Atmospheres*, 125, e2019JD032269, <https://doi.org/10.1029/2019JD032269>, 2020.
- Lloyd-Hughes, B. and Saunders, M. A.: A drought climatology for Europe, *International Journal of climatology: a journal of the royal meteorological society*, 22, 1571–1592, <https://doi.org/10.1002/joc.846>, 2002.
- 650 Lloyd-Hughes Benjamin and Saunders Mark A.: A drought climatology for Europe, *International Journal of Climatology*, 22, 1571–1592, <https://doi.org/10.1002/joc.846>, 2002.
- Martens, B., Miralles, D. G., Lievens, H., van der Schalie, R., de Jeu, R. A. M., Fernández-Prieto, D., Beck, H. E., Dorigo, W. A., and Verhoest, N. E. C.: GLEAM v3: satellite-based land evaporation and root-zone soil moisture, *Geoscientific Model Development*, 10, 1903–1925, <https://doi.org/10.5194/gmd-10-1903-2017>, 2017.
- 655 McKee, T. B., Doesken, N. J., Kleist, J., et al.: The relationship of drought frequency and duration to time scales, in: *Proceedings of the 8th Conference on Applied Climatology*, vol. 17, pp. 179–183, American Meteorological Society Boston, MA, 1993.
- Miralles, D. G., Holmes, T. R. H., De Jeu, R. a. M., Gash, J. H., Meesters, A. G. C. A., and Dolman, A. J.: Global land-surface evaporation estimated from satellite-based observations, *Hydrology and Earth System Sciences*, 15, 453–469, <https://doi.org/10.5194/hess-15-453-2011>, 2011.
- 660 Mo, K. C.: Drought onset and recovery over the United States, *Journal of Geophysical Research: Atmospheres*, 116, <https://doi.org/10.1029/2011JD016168>, 2011.
- Moravec, V., Markonis, Y., Rakovec, O., Svoboda, M., Trnka, M., Kumar, R., and Hanel, M.: Europe under multi-year droughts: how severe was the 2014–2018 drought period?, *Environmental Research Letters*, 16, 034062, <https://doi.org/10.1088/1748-9326/abe828>, 2021.
- Muñoz-Sabater, J., Dutra, E., Agustí-Panareda, A., Albergel, C., Arduini, G., Balsamo, G., Boussetta, S., Choulga, M., Harrigan, S., Hersbach, H., Martens, B., Miralles, D. G., Piles, M., Rodríguez-Fernández, N. J., Zsoter, E., Buontempo, C., and Thépaut, J.-N.: ERA5-Land: a state-of-the-art global reanalysis dataset for land applications, *Earth System Science Data*, 13, 4349–4383, <https://doi.org/10.5194/essd-13-4349-2021>, 2021.
- Naumann, G., Spinoni, J., Vogt, J. V., and Barbosa, P.: Assessment of drought damages and their uncertainties in Europe, *Environmental Research Letters*, 10, 124013, <https://doi.org/10.1088/1748-9326/10/12/124013>, 2015.
- 670 O, S. and Orth, R.: Global soil moisture data derived through machine learning trained with in-situ measurements, *Scientific Data*, 8, 1–14, <https://doi.org/https://doi.org/10.1038/s41597-021-00964-1>, 2021.
- Parry, S., Prudhomme, C., Wilby, R. L., and Wood, P. J.: Drought termination: Concept and characterisation, *Progress in Physical Geography: Earth and Environment*, 40, 743–767, <https://doi.org/10.1177/0309133316652801>, 2016.
- Rakovec, O., Samaniego, L., Hari, V., Markonis, Y., Moravec, V., Thober, S., Hanel, M., and Kumar, R.: The 2018–2020 Multi-Year Drought Sets a New Benchmark in Europe, *Earth’s Future*, 10, e2021EF002394, <https://doi.org/10.1029/2021EF002394>, 2022.
- 675 Rodell, M., Houser, P. R., Jambor, U., Gottschalck, J., Mitchell, K., Meng, C.-J., Arsenault, K., Cosgrove, B., Radakovich, J., Bosilovich, M., Entin, J. K., Walker, J. P., Lohmann, D., and Toll, D.: The Global Land Data Assimilation System, *Bulletin of the American Meteorological Society*, 85, 381–394, <https://doi.org/10.1175/BAMS-85-3-381>, 2004.
- Schneider, D. P., Deser, C., Fasullo, J., and Trenberth, K. E.: Climate data guide spurs discovery and understanding, *Eos, Transactions American Geophysical Union*, 94, 121–122, <https://doi.org/10.1002/2013eo130001>, 2013.
- 680



- Seager, R., Nakamura, J., and Ting, M.: Mechanisms of Seasonal Soil Moisture Drought Onset and Termination in the Southern Great Plains, *Journal of Hydrometeorology*, 20, 751–771, <https://doi.org/10.1175/JHM-D-18-0191.1>, 2019.
- Seneviratne, S., Zhang, X., Adnan, M., Badi, W., Dereczynski, C., Di Luca, A., Ghosh, S., Iskandar, I., Kossin, J., Lewis, S., Otto, F., Pinto, I., Satoh, M., Vicente-Serrano, S. M., Wehner, M., , and Zhou, B.: Weather and Climate Extreme Events in a Changing Climate. In *Climate Change 2021: The Physical Science Basis. Contribution of Working Group I to the Sixth Assessment Report of the Intergovernmental Panel on Climate Change*, Cambridge University Press, Cambridge, United Kingdom and New York, NY, USA, 2, 1513–1766, <https://doi.org/10.1017/9781009157896.013>, [Masson-Delmotte, V., P. Zhai, A. Pirani, S.L. Connors, C. Péan, S. Berger, N. Caud, Y. Chen, L. Goldfarb, M.I. Gomis, M. Huang, K. Leitzell, E. Lonnoy, J.B.R. Matthews, T.K. Maycock, T. Waterfield, O. Yelekçi, R. Yu, and B. Zhou (eds.)], 2021.
- 685
- 690 Shah, D. and Mishra, V.: Drought onset and termination in India, *Journal of Geophysical Research: Atmospheres*, 125, e2020JD032 871, <https://doi.org/https://doi.org/10.1029/2020JD032871>, 2020.
- Sheffield, J., Goteti, G., and Wood, E. F.: Development of a 50-year high-resolution global dataset of meteorological forcings for land surface modeling, *Journal of climate*, 19, 3088–3111, <https://doi.org/10.1175/JCLI3790.1>, 2006.
- Sousa, P. M., Barriopedro, D., García-Herrera, R., Ordóñez, C., Soares, P. M. M., and Trigo, R. M.: Distinct influences of large-scale circulation and regional feedbacks in two exceptional 2019 European heatwaves, *Communications Earth & Environment*, 1, 1–13, <https://doi.org/10.1038/s43247-020-00048-9>, 2020.
- 695
- Spinoni, J., Naumann, G., Vogt, J., and Barbosa, P.: European drought climatologies and trends based on a multi-indicator approach, *Global and Planetary Change*, 127, 50–57, <https://doi.org/10.1016/j.gloplacha.2015.01.012>, 2015.
- Trenberth, K. E.: Changes in precipitation with climate change, *Climate Research*, 47, 123–138, <https://doi.org/10.3354/cr00953>, 2011.
- 700
- Van Loon, A. F., Stahl, K., Di Baldassarre, G., Clark, J., Rangecroft, S., Wanders, N., Gleeson, T., Van Dijk, A. I. J. M., Tallaksen, L. M., Hannaford, J., Uijlenhoet, R., Teuling, A. J., Hannah, D. M., Sheffield, J., Svoboda, M., Verbeiren, B., Wagener, T., and Van Lanen, H. A. J.: Drought in a human-modified world: reframing drought definitions, understanding, and analysis approaches, *Hydrology and Earth System Sciences*, 20, 3631–3650, <https://doi.org/10.5194/hess-20-3631-2016>, 2016.
- Vicente-Serrano, S. M., Beguería, S., and López-Moreno, J. I.: A Multiscalar Drought Index Sensitive to Global Warming: The Standardized Precipitation Evapotranspiration Index, *Journal of Climate*, 23, 1696–1718, <https://doi.org/10.1175/2009JCLI2909.1>, 2009.
- 705
- Vicente-Serrano, S. M., Domínguez-Castro, F., Murphy, C., Hannaford, J., Reig, F., Peña-Angulo, D., Trambly, Y., Trigo, R. M., Mac Donald, N., Luna, M. Y., Mc Carthy, M., Van der Schrier, G., Turco, M., Camuffo, D., Noguera, I., García-Herrera, R., Becherini, F., Della Valle, A., Tomas-Burguera, M., and El Kenawy, A.: Long-term variability and trends in meteorological droughts in Western Europe (1851–2018), *International Journal of Climatology*, 41, E690–E717, <https://doi.org/10.1002/joc.6719>, 2021.
- 710
- Wilhite, D. A.: Drought as a natural hazard: concepts and definitions, in: *Drought: A Global Assessment*, Vol. I, edited by Wilhite, D. A., chap. 1, pp. 3–18, London: Routledge, <https://digitalcommons.unl.edu/droughtfacpub/69/>, 2000.
- Wilks, D. S.: *Statistical methods in the atmospheric sciences*, vol. 100, Academic press, 2011.
- Řehoř, J., Brázdil, R., Trnka, M., Lhotka, O., Balek, J., Možný, M., Štěpánek, P., Zahradníček, P., Mikulová, K., and Turňa, M.: Soil drought and circulation types in a longitudinal transect over central Europe, *International Journal of Climatology*, 41, E2834–E2850, <https://doi.org/10.1002/joc.6883>, 2021.
- 715